CRANFIELD UNIVERSITY

PETER HILLIS

COMBINED COAGULATION AND MEMBRANE MICROFILTRATION FOR REMOVAL OF NATURAL ORGANIC MATERIAL (NOM)

SCHOOL OF INDUSTRIAL AND MANUFACTURING SCIENCES

MPhil THESIS

CRANFIELD UNIVERSITY

SCHOOL OF INDUSTRIAL AND MANUFACTURING SCIENCES

MPhil THESIS

Academic Year 1998 – 1999

PETER HILLIS

COMBINED COAGULATION AND MEMBRANE MICROFILTRATION FOR REMOVAL OF NATURAL ORGANIC MATERIAL (NOM)

Supervisor: Dr. Simon Judd

March 1999

This thesis is submitted in partial fulfilment of the requirements for the Degree of

Master of Philosophy

ABSTRACT

The removal of natural organic matter (NOM) is a key requirement of many processes in potable water treatment. Conventionally, removal of NOM and colloidal material has been achieved by coagulation with inorganic coagulants followed by either direct rapid gravity filtration alone or clarification (sedimentation or flotation) followed by at least one stage of rapid gravity filtration.

An alternative to conventional processes is to combine membrane microfiltration (MF) with coagulation for NOM removal. The advantages of MF technology over traditional sand filters is the maintenance of an absolute barrier throughout the filtration process, thereby enhancing the physical separation process by presenting an absolute barrier to suspended materials. This thesis presents the results from such a system.

A 9.6m^2 hollow fibre hydrophilic polysulphone MF membrane system was used in combination with ferric sulphate under controlled pH conditions. The system was operated under constant flow condition and the coagulant concentration varied to assess performance. Coagulation conditions which promoted rapid aggregation of particles was found to give best performance with respect to pressure development, this coincided with a zeta potential at or near zero. Also, a pre-flocculation time of 20 seconds was found to be sufficient to allow complete removal of material associated with the coagulation process. Comparison with other workers showed similar results for the specific cake resistance despite considerable differences in both the scale and type of system used.

ACKNOWLEDGEMENTS

I would like to thank:

North West Water Ltd for sponsoring this work, in particular Dr. Roger Ford, Mr. Geoff Taylor and Dr. Martin Padley.

Dr. Simon Judd for his guidance during the supervision of this work.

My wife Jo, for her encouragement and support.

My two daughters Claudia and Mollie for their inspiration.

TABLE OF CONTENTS

APPENDICES 101

List of Figures

List of Tables

List of Symbols

Symbol	Description	Dimension
δ	Boundary layer thickness	m
α	Constant (Eq.9)	
ρ	Density	kgm^{-3}
θ	Pore tortuosity	
ζ	Zeta Potential	mV
η_0	Viscosity	$kgm^{-1}s^{-1}$
δc	Cake layer thickness	m
ε_c	Cake porosity	
ϕ_c	Volume fraction of solids in cake	
δ_m	Membrane thickness	m
Δp	Pressure drop across membrane and cake	Pa
ϕ_s	Volume fraction of solids in suspension	
A	Area	m^2
C_d	Cake concentration	$mol\ m^{-3}$
C_r	Retentate concentration	$mol\ m^{-3}$
D	Diffusion co-efficient	m^2s^{-1}
d_p	Particle diameter	m
f	Friction factor	
h	Time	hours
J	Flux	ms^{-1}
k	Mass transfer coefficient (Eq.3)	ms^{-1}

k_s	Filtration constant (Eq.19)	
l	Volume	litres
m	Area	m
p	Pressure	Pa
p_i	Inlet pressure	Pa
p_o	Outlet pressure	Pa
p_p	Permeate pressure	Pa
p_{tm}	Trans-membrane pressure	Pa
Q_p	Permeate flow	l/h
r	Radius	m
R'_c	Specific cake resistance (mass basis)	mkg^{-1}
$\hat{R}_c$	Specific cake resistance	m^{-2}
R_{bl}	Boundary layer resistance	m^{-1}
R_c	Cake layer resistance	m^{-1}
R_f	Fouling layer resistance	m^{-1}
R_g	Gel layer resistance	m^{-1}
R_m	Membrane resistance	m^{-1}
t	Time	s
μM	Concentration	
V	Volume	m^3

List of Abbreviations

AIDS	Acquired Immune Deficiency Syndrome
AWWA	American Water Works Association
BSA	Bovine Serum Albumen
CF	Crossflow
DAF	Dissolved Air Flotation
DE	Dead-end
DOC	Dissolved Organic Carbon
DWI	Drinking Water Inspectorate
ESWTR	Enhanced Surface Water Treatment Rule
EU	European Union
FTIR	Fourier Transform InfraRed
GAC	Granular Activated Carbon
GLC	Gas-Liquid Chromatography
HAA	Halo Acetic Acid
ICP	Inductively Coupled Plasma
MF	Microfiltration
MW	Molecular Weight
MWCO	Molecular Weight Cut Off
NF	Nanofiltration
NOM	Natural Organic Material
NWW	North West Water Ltd
PAC	Powdered Activated Carbon
PACl	Poly Aluminium Chloride

PCV	Prescribed Concentration or Value
PDA	Photometric Dispersion Analyser
RO	Reverse Osmosis
SCD	Streaming Current Detector
SWTR	Surface Water Treatment Rule
THM	Tri-Halo Methane
THMFP	Tri-Halo Methane Formation Potential
TMP	Trans Membrane Pressure
TOC	Total Organic Carbon
TSS	Total Suspended Solids
UF	Ultrafiltration
UK	United Kingdom
WHO	World Health Organisation

1.0 INTRODUCTION

The water treatment works at which this work was carried out is located at Longridge just outside Preston in Lancashire. The works draws its water from Alston No.3 reservoir, which is fed by from Alston reservoirs 1 and 2 and Spade Mill reservoirs 1 and 2. The water received by the works has a low alkalinity, low turbidity and contains coloured or natural organic material (NOM), which is typical of surface derived water from this area. The range of raw water quality is shown in Table 1.1.

Table 1.1. Summary of raw water quality 1992 to 1998

	pH	Colour (Hz)	Turbidity (NTU)	Alkalinity (mg/l as CaCO3)	Manganese (ug/l)	Aluminium (ug/l)	Iron (ug/l)
Mean	7.44	15.6	0.89	12	13.7	68.0	56.3
Max	8.84	34	4	25	76.5	460	474
Min	5.96	3	0.1	6	1	20	8

As a result of the organic content of this supply, North West Water Ltd (NWW) has been required to apply physio-chemical treatment in order to comply with the current water regulations (Section1.1.2). The current treatment consists of microstraining to 90μm followed by disinfection with chlorine and pH elevation using lime.

In recent years water produced and supplied by this works has resulted in failure of the trihalomethane (THM) standard. The strategy adopted by NWW to ensure compliance with the regulations has been to apply a coagulation based process followed by physical

separation to remove the NOM precursors to THM formation prior to addition of chlorine.

1.1 Water Quality & Legislation

1.1.1 Natural Organic Material (NOM)

The presence of NOM in surface waters impacts on many of the processes used in potable water treatment. This organic matter, which may be soluble or insoluble, originates from the degradation of vegetable matter. The majority of the soluble material is in the form of colloidal humic material and the more soluble fulvic acids and carbohydrates. Also present are small and very soluble organic molecules such as carboxylic and amino acids. The insoluble particulate material usually constitutes a small fraction of the total.

NOM presents two main problems in water treatment. Firstly, they give water its colour, which is undesirable on aesthetic grounds. Secondly, upon contact with chlorine, which is used for disinfection, they lead to the generation of halogenated organic by-products, ultimately yielding THMs. Both colour and THM have limits stipulated by the EC drinking water regulations (Section 1.1.2). Also, the presence of NOM exerts a significant chlorine demand and can thus reduce disinfection efficacy.

1.1.2 Trihalomethanes

In Europe, the 1989 European Union (EU) Directive on drinking water quality promulgated quality standards for potable water covering microbiological and chemical parameters (DoE, 1989). These standards have been incorporated into UK legislation as prescribed concentration or values (PCVs). The PCV for coloured material in drinking water was set at 20 degrees hazen (°Hz). Chlorination of NOM forms a series of by-products, originally known as THM and a PCV of a 100ug/l three month rolling average in the distribution zones (as recorded at the customers tap) is the current UK standard. More recently the EU has reviewed this limit of a 100µg/l three month rolling average and has amended the standard to be an absolute rather than an average measure (98/83EC). Also, a new set of chlorination by-products of humic material such as haloaceticacids (HAA) have been identified which will be incorporated into future EU legislation. The regulations are being tightened in line with improving analytical techniques and the completion of World Health Organisation (WHO) toxicological assessment of individual chlorination by-products (WHO, 1993). The issue of whether existing water treatment processes can economically meet these standards or whether additional treatment will be required is now vexing the European water industry.

1.1.3 Cryptosporidium

The protozoan parasite *Cryptosporidium* was first noted early in this century, although its association with human disease did not arise until 1976. Thereafter, it has become more recognised as a causative agent of gastro-enteritis, initially in immuno-compromised or immuno-suppressed people (e.g., AIDS sufferers or transplant

patients), but more recently in persons with normal immune systems. *Cryptosporidium* infects a wide range of vertebrates, including most domestic animals, typically affecting the very young. Cross-species transfer of the parasite occurs and humans of all ages have proved susceptible.

There are at least 4 recognised species, although *Cryptosporidium Parvum* is the only one known to infect humans. *Cryptosporidium* grows and reproduces within the host digestive organs and has been observed in the respiratory tract, particularly in birds. The entire life cycle takes place within one host. Oocysts, which are resistant to many environmental stresses, are then shed in the faeces of the affected individual. Subsequent ingestion of the oocysts by a potential host may result in a new infection (faecal-oral route of transmission). Transmission to humans is therefore by person-person or animal-person contact, ingestion of contaminated water or food, or by contact with contaminated objects; the relative importance of these routes is not known.

Studies have shown that *Cryptosporidium* is not completely killed or rendered non-viable at normal concentrations of conventional disinfectants used in the water treatment process, such as chlorine, ozone or chlorine dioxide (Finch *et al*, 1997). It is also not reliably removed by conventional sand filtration, as experience has demonstrated (Sections 1.1.2.1-1.1.2.2)

1.1.3.1 Waterborne Outbreaks

In 1993 the population of Milwaukee, Wisconsin was affected by an increase in diahorreal illness (Solo-Gabriele, 1996). It was reported that up to 400,000 inhabitants of the city were affected. The drinking water supply was identified as the source of the illness and *Cryptosporidium parvum* was shown to be the major cause of the complaint. A number of imuno-comprimised people were reported to have died as a result of contracting the illness.

The importance of *Cryptosporidium* as concern to public health was demonstrated most recently in Sydney, Australia in July 1998. In this case nearly 4 million people were required to boil their drinking water as a result of the organism entering the water supply. The financial cost to the Water Company in this instance will be in the order of tens of millions of pounds, but more the loss of public confidence in the drinking water and the Water Company cannot be quantified. A summary of UK waterborne outbreaks of cryptosporidiosis is presented in Table 1.2.

Table 1.2. UK outbreaks of cryptosporidiosis associated with water supplies April 1988 – April 1998 (Bouchier, 1998)

Date	Source/Treatment	Oocysts In Raw Water	Number Of Cases	Association With Water	Conclusions/Comments
April 88	Surface water with Coagulation and filtration	Yes	27	Strong	Agricultural slurry contamination of water in distribution
Mar 89	Impounded reservoir supply with coagulation and filtration	Yes	500+	Strong	Contamination of source water with animal wastes, breakthrough of treatment
Mar 89	Surface water, coagulation, filtration	Yes	See above	Strong	River flows abnormally low, severe diarrhoea in cattle upstream of intake
Apr 89	Surface water, no filtration	Yes	244	Probable	Unfiltered water, potential source of discharge from sewage treatment works and farm drains and non-point discharge from grazing animals
Dec 89	Lowland river with bankside storage, roughing filters and slow sand filters	No	477	Strong	Outbreak followed bypassing of filters

Date	Source/Treatment	Oocysts In Raw Water	Number Of Cases	Association With Water	Conclusions/Comments
Dec 90	Lowland tidally influenced river, direct abstraction, filtration	No	47	Probable	Rapid fluctuations in source water quality at time of outbreak
Apr 91	Spring, well and stream supply, crude filtration	No	5	Possible	Possible agricultural contamination of well supply, inadequate treatment
Apr 92	Surface water, no filtration	Yes	50	Probable	Unfiltered water, Potential point source discharge from sewage treatment works and farm drains and non-point discharge from grazing animals
Jul 92	Lowland river with direct abstraction, separation process and bankside filtration with no filtration	No	108	Probable	Possible link with groundwater turbidity
Nov 92	Upland reservoir and surface water supplying aqueduct, slow sand filtration	Yes	125	Strong	Heavy rainfall in the catchment, high raw water turbidity, increase in filtered water turbidity
Nov 92	Groundwater, no filtration	No	47	Probable	Outbreak probably caused by faecal contamination from cattle housed adjacent to wellhead
Apr 93	Stream source, no filtration	Yes	3	Probable	Inadequate treatment, source open to potential animal contamination
Apr 93	Groundwater from fissured strata, no filtration	No	40	Probable	Outbreak possibly caused by rapid recharge of surface water contaminated with oocysts
Apr 93	Upland reservoir, no filtration	No	48	Probable	Possible run-off from grazing, very heavy rainfall
Jun 93	Upland reservoir and surface water supplying aqueduct, slow sand filtration	No	97	Probable	Outbreak caused by poor operating practices and excessive head on filters
Jun 94	Spring fed natural impoundment, upflow filtration	No	8	Probable	Possible animal contamination following heavy rain
Feb 95	Spring supply, no filtration	No	40	Strong	Heavy rain washed in waste animal material
Aug 95	Lowland river with direct abstraction, separation process and bankside infiltration with no filtration	Yes	575	Strong	Plant operating above design output, evidence of turbidity peaks in bankside infiltration water
Jan 96	Lowland river with coagulation and filtration	Yes	126	Strong	Outbreak occurred when works was under strain with excess flow causing solids breakthrough
Mar 96	Surface water with bankside storage, filtration, no coagulation	No	20	Probable	Outbreak caused by breakthrough of solids as a result of inadequate treatment during an algal bloom
Apr 96	Lowland river with full treatment	No	80	Probable	Probable association with water but no evidence of plant operation problems
Feb 97	Groundwater from fissured strata, no filtration	Yes	345	Probable	Outbreak caused by infiltration of surface water containing oocysts
Feb 97	Lowland river, coagulation and filtration	No	22	Probable	Outbreak possibly associated with turbidity peak in filtered water
May 97	Spring supply, partial filtration	No	34	Possible	Possible run-off from spring grazing
Apr 98	Surface water, no filtration	Yes	303	Possible	Unfiltered water, potential point source discharge from sewage treatment works and farm drains and non-point discharge from grazing animals

1.1.3.2 Water Treatment for the Removal of *Cryptosporidium*

The information summarised in Table 1.2 clearly shows that conventional treatment processes are susceptible to the passage of *Cryptosporidium* into the drinking water supply. The American Water Works Association (AWWA) has commissioned a number of investigations into the removal of the organism by conventional processes and found varying degrees of success. What is apparent is that conventional sand filtration allows oocysts to pass during certain periods of operation (Patania *et al*, 1995) and if this coincides with a significant challenge then large numbers can enter the potable water and present a risk to public health.

The ability of microfiltration (MF) and ultrafiltration (UF) systems to remove a range of micro-organisms, such as *Giardia*, *Cryptosporidium* and bacteria has been demonstrated in a number of studies (Jacangelo, 1991, Jacangelo, 1992, Yoo, 1995 and Jacobs, 1997). Changes in US regulation, the surface water treatment rule (SWTR) and the enhanced surface water treatment rule (ESWTR), set out criteria for the removal of *Cryptosporidium* that conventional treatment will find difficult to reliably comply with. This resulted in the need for a simple technology able to remove micro-organisms whilst still being cost-competitive with conventional treatment. With *Cryptosporidium* oocysts being between 4 and 6 um in size the use of either a MF or UF membrane provide an absolute barrier to the organism. The fact that a number of companies already have available MF and UF systems with operational experience of plant at a large enough scale to satisfy the needs of water supply companies makes it possible for the technology to be adopted rapidly.

1.1.3.3 UK Guidelines and Regulation

Recent outbreaks of cryptosporidiosis in the UK, most notably the Swindon-Oxford incident of 1989, have forced UK water companies to examine the use of membranes to alleviate public health concerns. UK guidelines, in the form of the Badenoch Reports (1990 and 1995) and Bouchier Report (1998), have not been prescriptive: it has been suggested (Taylor *et al*, 1998) that application of appropriate technology by the UK water companies arises from an assessment of the risk of contamination of raw water supplies with the adequacy of treatment. However, a proposed addition to the UK Water Regulations is the imposition of a numeric standard for the UK of <0.1 oocysts/litre. This is the first numeric standard to be adopted world-wide and means that the UK now has the most stringent standard for *Cryptosporidium* in the world.

1.2 Process Selection Rationale

The traditional solution for the removal of NOM involves the use of direct filtration, sedimentation and gravity filtration or DAF and gravity filtration (section 2.2). Each of these processes can meet the required treatment targets for colour and the current THM target. However, they have little flexibility in their operation and are fully developed technologies with little scope for further development. A more novel approach is the application of membrane technology to removal of NOM (Jacangelo *et al*, 1995). Membranes are at a relatively early stage in their development for water treatment and there is considerable scope for both performance improvements and further reductions in manufacturing costs. Moreover, the modular nature of membrane treatment processes allows for future increases in capacity.

The removal of NOM by membranes can be achieved by molecular weight exclusion using nanofiltration (NF) (Taylor, 1995). Application of MF to this duty on the other hand demands pre-treatment with an inorganic coagulant (Laine *et al*, 1990). There are a number of advantages of using MF as opposed to NF. MF operates at much lower pressures and requires only minor pre-treatment of the raw water, such as coarse microstraining to 200μm followed by the chemical dosing. Investigations on raw waters and effluents have demonstrated that pre-treatment with flocculating agents can reduce fouling and increase membrane flux and permeate quality (Ben Aim *et al*, 1988). Waste streams can be more easily managed using conventional and existing facilities, and the final water requires only residual disinfection and pH correction.

As far as comparison with conventional treatment is concerned MF offers significant advantage in the barrier nature of the process, both with respect to NOM and in particular to infectious micro-organisms. Since oocysts of *Cryptosporidium* are approximately 4 to 6μm in size then a MF system with an average pore size 0.1μm would be expected to present an absolute barrier to passage as long as the integrity of the system is maintained. The barrier is maintained at all stages of the process unlike sand filters, which have been shown to pass large amounts of particles immediately after backwash (Hillis and Colton, 1995), because such depth filtration processes rely ostensibly upon adsorptive removal rather than the sieving mechanism of MF.

1.3 Objectives

The objectives of this work are to:

- demonstrate the efficacy of combining coagulation and microfiltration for potable water treatment to remove NOM and consequently meet water quality standards for THM, and
- develop an understanding of the relationship between coagulation conditions and operational performance.

2.0 LITERATURE REVIEW

2.1 Potable Water Treatment for the Removal of NOM

2.1.1 Chemical Treatment

Removal of NOM from surface waters has been a long-standing objective of water treatment processes. Conventionally removal has involved the addition of between 0.01mM and 0.30mM as trivalent metal inorganic coagulants, such as aluminium or ferric sulphates. Such chemical dosing is followed by the removal of the suspended coagulated material by a range of separation processes, the most common of which are outlined below.

2.1.2 Direct rapid gravity filtration

Following addition of the metal coagulant, water is passed through a filter containing a medium such as sand, anthracite, granular activated carbon (GAC) or most usually a combination of sand and anthracite. The filter bed presents a plug flow reactor in which numerous interactions between the medium and the "floc" particles (flocculated material formed as a result of coagulation) take place. Flocculated material is transported and attaches to the filter medium via a number of mechanisms, dictated by the system hydrodynamics, particle and grain size and surface chemistry.

As more and more material is deposited on the filter medium the resistance to filtration or headloss increases and detachment of floc can occur. This phenomenon is known as

"breakthrough", and the filter must be cleaned prior to breakthrough if the operational performance integrity is to be maintained. A backwashing process, which can be typically every 24 hours, achieves cleaning. Upon returning to service the filter goes through a maturation period, or "ripening", before optimum performance is achieved (Hillis and Colton, 1995).

2.1.3 Sedimentation and rapid gravity filtration

Coagulated water is fed into the base of a tank at such a rate as to facilitate flocculation and also to allow floc particles to settle. At a suitable up-flow rate the settling floc will amass to form a dense layer of flocculated material, known as a "floc-blanket", and this will further aid the removal of coagulated material. The clear water passes through this blanket and is decanted off at the surface before further treatment by passage through rapid gravity filters to remove any material that is carried through the sedimentation tank. Excess sludge from the blanket is removed periodically to limit its accumulation.

2.1.4 Dissolved Air Flotation (DAF) and rapid gravity filtration

A pressurised air-saturated water stream, making up 10% of the forward flow, is introduced into a tank via an arrangement of nozzles or needle valves over which previously flocculated water passes. On depressurising this water small bubbles are formed which attach to the floc particles and result in their flotation to the surface of the tank. A thick sludge layer is formed on the surface, which is removed by mechanical scraping. The clear water passes under the floated sludge blanket and is further treated

using rapid gravity filtration, again to remove floc material not separated in the flotation tank.

2.2 Coagulation

Coagulation is a key part in the solid-liquid separation process and as such used in a number of industrial and municipal applications including water treatment. The term coagulation is used to describe the destabilisation of very small particles, usually of colloidal size (<1μm), if coagulation is sufficient the particles will attach to one another on collision to form aggregates which become visible at around 1mm or more. This aggregation phenomenon is known as flocculation. The separation of these aggregated particles from the liquid phase - a process given the general term clarification - yields a clear supernatant. As already outlined, clarification can be carried out by sedimentation, flotation or filtration.

The surfaces of colloidal particles that are dispersed in an aqueous medium normally carry a negative charge. The charge may arise from various surface phenomena; dissociation of surface ionic groups or preferential adsorption of ions or organic matter from solution. This charge produces electrostatic repulsion between like charged particles and so stabilising the dispersion. In order to reduce these repulsive forces to facilitate aggregation, a coagulant of opposite charge is usually added. Adsorption of the coagulants onto the surfaces of colloidal particles minimises the electrostatic repulsion between them resulting in destabilising of the dispersion. This then allows the ubiquitous attractive van der Waals forces to predominate and aggregation to occur.

Different chemical coagulants can achieve the destabilisation of small particles to form larger particles in different ways. The four governing mechanisms identified for coagulation comprise (Gregory, 1993):

- double-layer compression,
- charge neutralisation,
- enmeshment in a precipitate (sweep coagulation), and
- adsorption to permit interparticle bridging

The two mechanisms that are thought to predominate in water treatment are charge neutralisation and sweep coagulation.

2.2.1 Charge neutralisation

The universal attractive forces between atoms and molecules (van der Waals forces) also operate between particles and thus have a role in the interaction of colloidal material. As the particles move closer together the attraction increases until the particles are in contact whereby the attraction becomes infinitely strong. In reality, short-range repulsion forces prevent particles coming into true contact hence the attraction remains finite.

Since virtually all particles in aqueous solution carry a surface charge, oppositely charged ions (counter-ions) will be attracted to and so are associated with the surface. This produces a fixed layer of counter ions known as the "inner Helmholtz layer". An "outer Helmholtz layer" is then formed; comprising hydrated fixed counter ions.

Another region adjacent to the Helmholtz layers then comprises ions that are free to move. It is only at the outer boundary of this "diffuse layer" that the potential drops to zero (Figure 2.1).

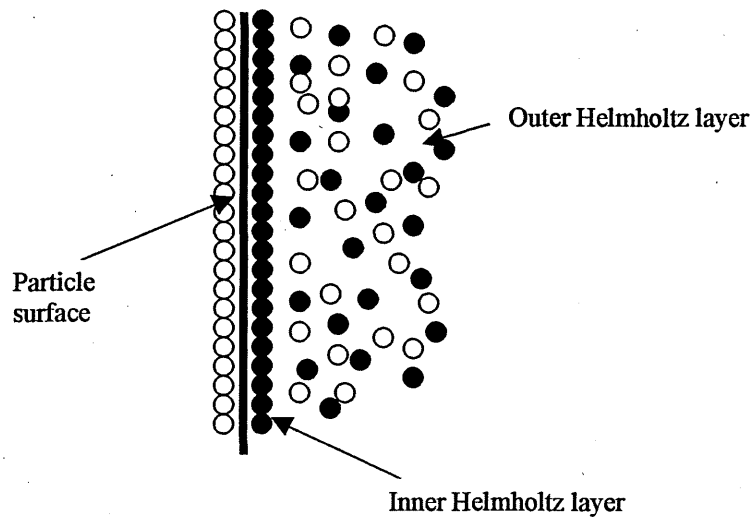

Figure 2.1 The electrical double layer according to the Helmholtz model, negative charge (O), positive charge (●)

The nature of the so-called electrical double-layer can exert a significant influence on the interaction between charged particles. At low ionic strengths the diffuse layer extends further than for higher electrolyte concentrations. Another important quantity in particle interaction is the electrical potential at the outer Helmholtz plane. This potential cannot be measured directly but it is believed to correspond to the zeta potential (ζ) (or "shear plane"), which can be obtained experimentally from electrokinetic techniques.

Increasing the ionic strength of a solution can be seen to have two effects on the electrical double layer interaction. Firstly, the thickness of the double layer is reduced so that particles can approach closer before repulsion has an effect. Secondly, zeta

potential is also decreased which reduces the magnitude of the repulsion at a given separation distance (Soderbaum, 1925).

When the particles zeta potential and the ionic strength of the solution is such that repulsion outweighs attraction a potential energy barrier exists which will limit contact between particles and hence aggregation. As the ionic strength is increased and/or zeta potential is decreased the energy barrier becomes lower and the contact between particles can occur more easily. At a certain electrolyte concentration the energy barrier disappears and particles can adhere upon collision. These particles are then fully destabilised and undergo rapid coagulation.

In adsorption destabilisation by conventional coagulants such as the trivalent salts of iron and aluminium it is the particle zeta potential which is directly affected by the coagulation chemicals. The coagulants form cationic products which are adsorbed on to the surface of the oppositely charged (negative) particles, decreasing the zeta potential and so promoting aggregation between the particles. Control of coagulant addition is very important since excess can result in the surface charge being reversed and the suspension restabilising.

2.2.2 "Sweep" coagulation

Under certain conditions of pH and concentration of coagulant and supporting inert electrolytes, the metal hydroxide will precipitate (Figure 2.2). For example, according to Figure 2.2, a 10^{-4} M solution of Fe (III) can precipitate amorphous Fe $(OH)_3$ above a pH value of 3. As the precipitate forms colloidal particles can become enmeshed within it

and this has thus become known as "sweep" coagulation. It has been recognised for some time (O'Melia, 1969) that sweep coagulation removes mostly insoluble material i.e. suspended solids, although adsorption of dissolved matter on to the surface of the floc material may also occur.

2.2.3 Coagulation with Iron salts

Coagulants in the iron (III) form undergo a pH dependent hydrolysis reaction (Table 2.1) to form hydrolysed species. At low pH levels <6.2, the dominant soluble species are cationic monomers such as Fe^{3+} and $Fe(OH)^{2+}$ (Figure 2.2). Given that equilibrium thermodynamics, as expressed in Table 2.1 and Figure 2.2, dictates that Fe(III) is highly insoluble at intermediate pH values – almost 10^{-11} moles/l (~0.5ppb) at pH 8, it stands to reason that in practice it is the kinetics of reactions in water that govern the efficiency of Fe(III) addition in potable water treatment.

Table 2.1. Reactions during hydrolysis of Fe(III) (Johnson and Amirtharajah, 1983)

Reaction	log K (25°C)
$Fe^{3+} + H_2O = FeOH^{2+} + H^+$	-2.2
$FeOH^{2+} + H_2O = Fe(OH)_2^+ + H^+$	-3.5
$Fe(OH)_2^+ + H_2O = Fe(OH)_3 + H^+$	-6
$Fe(OH)_3 + H_2O = Fe(OH)_4^- + H^+$	-10
$2Fe^{3+} + 2H_2O = Fe_2(OH)_2^{4+} + 2H^+$	-2.9
$3Fe^{3+} + 4H_2O = Fe_3(OH)_4^{5+} + +4H^+$	-6.3
$Fe(OH)_3(am) = Fe^{3+} + 3OH^-$	-38.7(estimated)
α - $FeO(OH) + H_2O = Fe^{3+} + 3OH^-$	-41.7

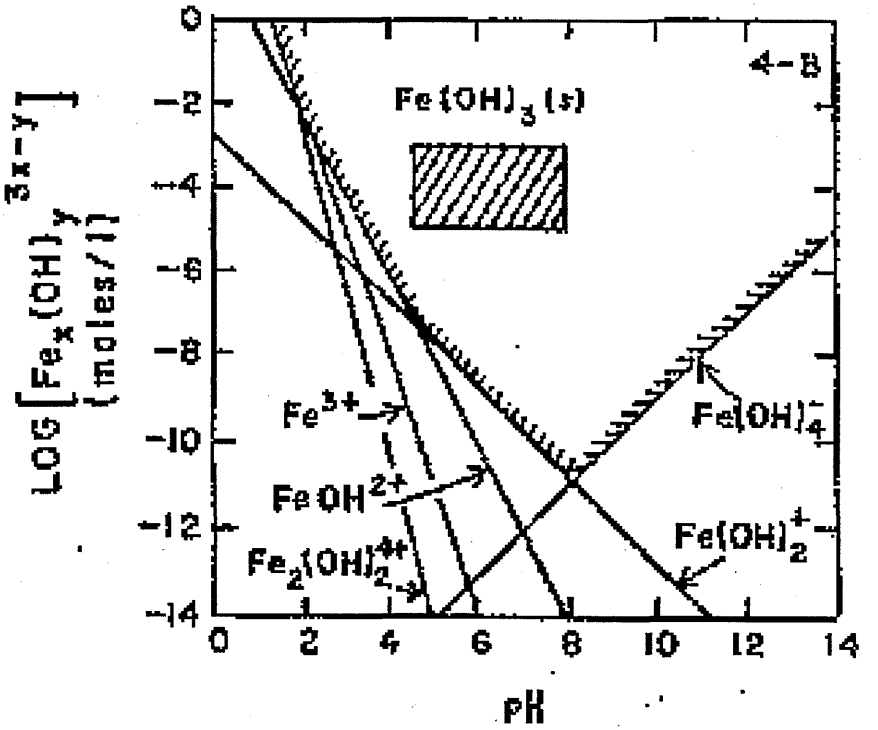

Figure 2.2 Solubility diagram for iron species in equilibrium with solid iron hydroxide (Dentel 1991)

Control of the chemical conditions of the coagulation process is important in determining the nature of the coagulant chemical reaction, i.e. neutralisation or precipitation. A useful tool for predicting the chemical conditions at which coagulation occurs is the coagulation diagram as originally constructed by Johnson and Amirtharajah (1983), (Figure 2.3), which relates specific chemical conditions, such as pH and concentration, with the two different mechanisms by which coagulation is achieved in water treatment. The diagram shows two distinct regions of coagulation using iron (III); charge neutralisation occurs at pH values <6.2 and sweep predominates when the pH is >6.2. This is due to the fact that at pH values of <6.2 the soluble species responsible for charge neutralisation, i.e. cationic monomers such as Fe^{3+} and Fe $(OH)^{2+}$, predominate. It is these species which have been identified with the removal of

organic material by the mechanism of direct precipitation via the formation of monomeric and small polymeric products (Semmens and Field, 1980, Randtke, 1988, Rebhun and Lurie, 1993,). Typical conditions for charge neutralisation comprise doses of iron (III) between ~0.036mM to 0.27mM and a pH range of ~5.0 to 6.0

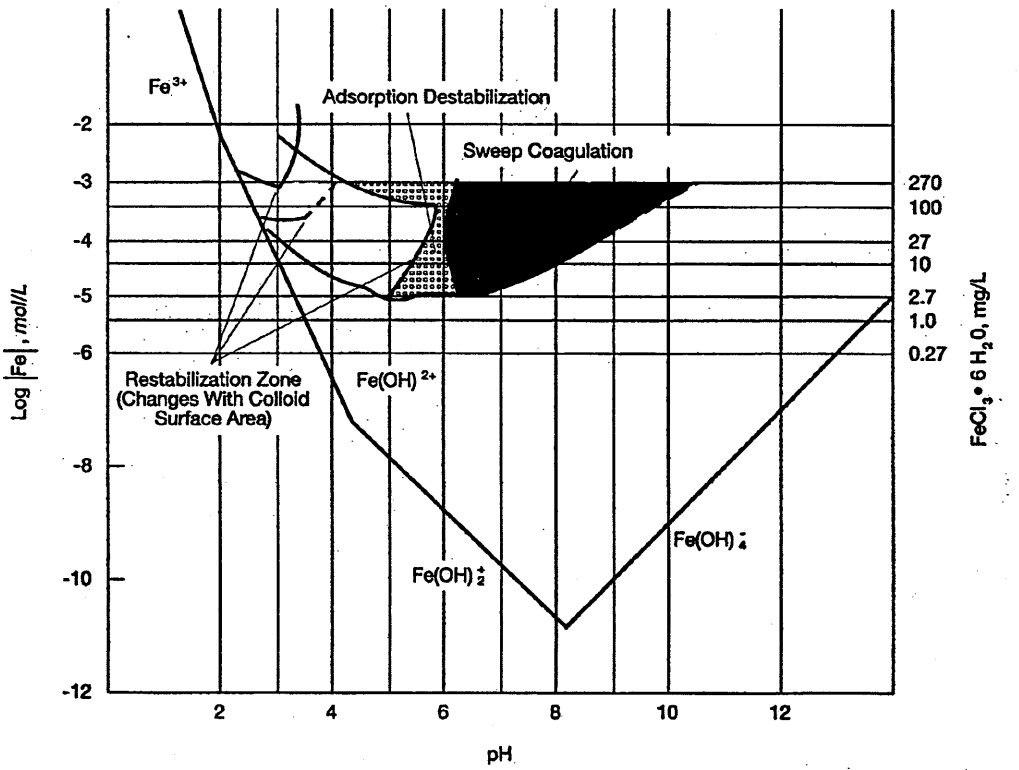

Figure 2.3. Design and operation diagram for Fe^{3+} coagulation (Johnson and Amirtharajah, 1983)

2.2.4 Kinetics of Coagulation

During the destabilisation of colloidal material by hydrolysed metal coagulants a number of hydrolysis products are formed (Table 2.1). The formation of these complexes occurs very rapidly, within microseconds for the monomeric species and within one second for the polymeric species (Hahn and Stumm, 1968). The formation of

iron hydroxide for entrapment of colloidal material by sweep coagulation is thought to be completed between one and seven seconds (Letterman *et al*, 1973). Therefore, for charge neutralisation to occur it is important to disperse the coagulation chemicals rapidly and evenly so that the hydrolysis products that develop within one second can be adsorbed onto the surface of colloids and particles and hence cause destabilisation and so promote aggregation.

The kinetics of the aggregation process is dependent on the frequency at which destabilised particles collide and also the efficiency of each collision. In the absence of an energy barrier to coagulation it can be assumed that every collision will lead to particle growth and hence aggregation. If convection is absent, then the coagulation process is controlled solely by the kinetics of the diffusion process that leads to particle-particle interaction. Coagulation, which occurs under the influence of Brownian motion, is called "perikinetic" coagulation.

The rate at which collisions occur can be enhanced, and thus the rate of coagulation increased, by introduction of hydrodynamic forces. These forces can be introduced either by rapid stirring (as in a jar-test) or by flow through a pipe at high shear rates. This is known as "orthokinetic" coagulation. Hydrodynamic or shear effects increase with increasing particle size and are dominant for particles of a few microns in size. If the initial particles are smaller than this then Brownian motion and hence perikinetic effects controls the early stages of coagulation (Everett, 1988).

2.2.5 Removal of NOM by Coagulation

The removal of NOM from water by coagulation using iron (III) based coagulants has been investigated extensively (O'Melia, 1969, Sinsabaugh, *et al*, 1986, Ying *et al*, 1988, Haarhof and Cleasby, 1988, Hong-Xiao and Stumm, 1987). It has been found that NOM is removed most effectively at pH values between 4.5 and 5.5, the removal being accomplished via the precipitation of Fe-humates. The precipitation is thought to result from cationic hydrolysis products causing charge neutralisation of colloidal humic material and therefore promoting aggregation (Randtke, 1988). Other reactions may also take place with other natural material present in raw waters such as suspended and colloidal inorganic matter (Tambo, 1998).

2.2.6 Optimisation of Coagulation Conditions

The most common tool used by water practitioners for the identification of "optimum" conditions for coagulation is the jar-tester (Hall and Hyde, 1992). A series of experiments are carried out over a range of metal coagulant concentrations and pH conditions on the raw water of interest. Once the jar-test has been completed the clarified water is decanted and filtered. These filtered samples are then analysed for measures of water purity such as organic material (colour) and metal coagulant residual. The point at which removal of colour is maximised and coagulant residual is minimised represents the "optimum". Figure 2.4 shows a correlation of colour residual against pH for incrementally increasing alum doses.

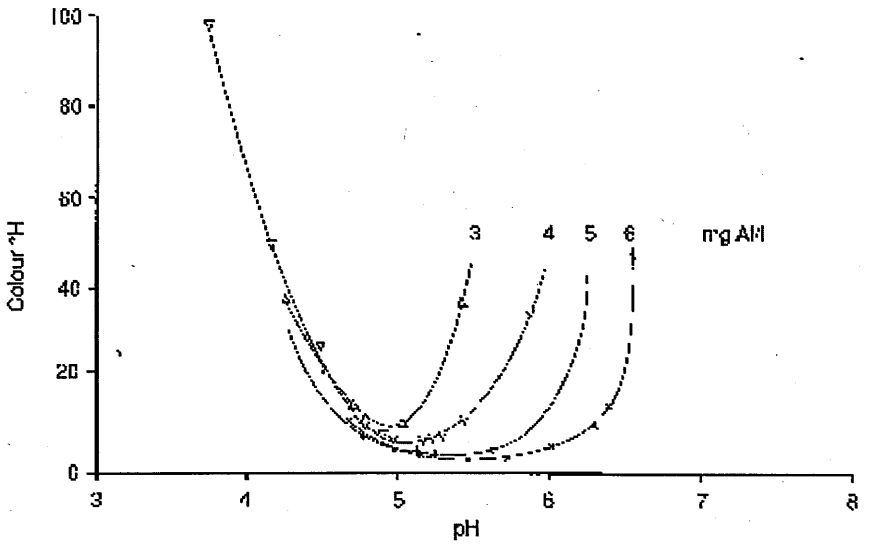

Figure 2.4 Effect of pH on optimum Al dose from jar-tests (Hall and Hyde, 1992)

A more recent innovation in determining "optimum" coagulation and flocculation conditions is the use of a Photometric Dispersion Analyser (PDA 2000) (Gregory and Hiller, 1995), which has been used to monitor the change in "flocculation index" (FI) with time and coagulant dose in combination with a jar-tester. The FI represents the fluctuations in the intensity of light transmitted through a flowing suspension. As particles aggregate the amplitude of the fluctuations increases giving an indication of the extent of flocculation. The FI then has a sigmoid relationship with time which varies according to the coagulant dose whilst still presenting the same asymptotic maximum value (Figure 2.5). The maximum slope, or flocculation rate, has been found to correlate well with the residual turbidity after a standard jar-test and settling procedure; the higher the value obtained for the rate of change of flocculation index the lower the residual turbidity.

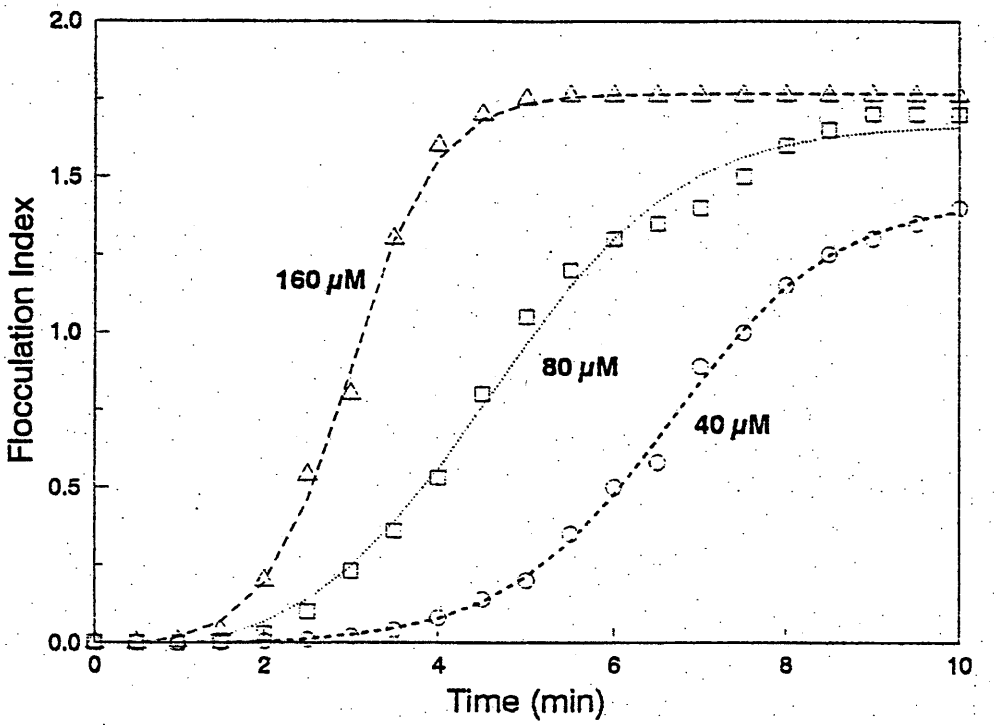

Figure 2.5 Flocculation index vs time for three ferric doses (Gregory and Hiller, 1995)

The FI technique represents an alternative on-line monitoring method to the standard jar.

A much better established technique is the Streaming Current Detector (SCD). This is based on measuring the electrokinetic charge carried by particles in the water, which is directly influenced by the action of coagulants. Where adsorption-charge neutralisation is the dominant mechanism for destabilisation of particles, or where dissolved organics are to be removed by cationic additives, the SCD technique can be very effective in determining the optimum coagulant dosage. It is less successful when charge neutralisation is less important, for instance in the cases of sweep flocculation.

Certain optical techniques for detecting the early growth of flocs, immediately after dosing, may also be useful, but these have not been thoroughly tested under treatment plant conditions.

2.3 Membrane Processes for Drinking Water Treatment

Major pollutants in water can be categorised as physical (turbidity, suspended solids, colour), chemical (dissolved metals, soluble organics, pesticides) and microbiological (bacteria, protozoa and viruses) in nature. The range of pollutants present in the feed water will determine the selection of the appropriate membrane process, since these processes vary significantly in their selectivity.

2.3.1 Reverse Osmosis

The use and diversity of application of membrane processes for municipal water treatment has increased significantly over the last 25 to 30 years. Regarding potable water production, the development of reverse osmosis (RO) membranes in large-scale applications has been largely based on their ability to remove dissolved salts from sea or brackish water (Pepper, 1992). More recently low-pressure RO membranes have been developed for nitrate and pesticide removal from groundwater (Murrer, 1996). RO systems operate at relatively high pressures, up to 20 bar depending on the osmotic pressure of the water to be filtered. Fairly comprehensive pre-treatment is required prior to entry into an RO system. The main objectives of any pre-treatment is to remove various materials which are responsible for "fouling", the general term given to the

accumulation of matter on or within a membrane which produces a decline in flux. The degree of pre-treatment is very much dependent on the quality of the feed water.

2.3.2 Nanofiltration

Nanofiltration (NF) membranes were primarily developed to soften brackish groundwaters as an alternative to RO membranes. NF systems are able to operate at lower pressures, 5 to 10 bar, than RO. The membranes themselves are capable of removing up to 90% of sulphate and total hardness and between 90 and 95% of dissolved organic material, both natural and polluting (Anselme *et al*, 1994). NF systems, like RO, require pre-treatment to control fouling by suspended solids and bacteria. The process is becoming a viable alternative to RO for partial salt removal due to the better conversion rates and lower operating pressures.

2.3.3 Ultrafiltration

The performance of an ultrafiltration (UF) membrane is defined by its "molecular weight cut off" (MWCO), the size being in Daltons. UF membranes of MWCO 1000 have been found to be capable of removing some of the coloured NOM found in raw waters. UF membranes with MWCO of between 500-800 Dalton, on the other hand, are able to remove 80% of dissolved organic carbon (DOC) whilst only slightly reducing the hardness (<10%) (Jacangelo, 1991). The main advantages of using a low MWCO UF membranes over an NF system are the reduced need for pre-treatment, lower pressures of operation (up to 2 bar) and the production of a non-aggressive product that does not require any post remineralisation before going into supply. There are a number

of UF systems operating on municipal water supplies, e.g. Tyn-y-Wan in South Wales, L'Apie in the South of France and Hull is East Yorkshire, these applications employ systems with a MWCO of between 50,000 and 100,000 Dalton.

2.3.4 Microfiltration

MF represents the membrane having the lowest energy demand, but also the lowest selectivity. Since the process primarily removes suspended matter. In terms of suspended (i.e. supra-colloidal) material the water produced by both UF and MF systems are identical. MF membranes will remove a maximum of 20% of total organic carbon (TOC) from most surface waters, representing the suspended organic fraction; no discernible removal of any soluble contaminants takes place (Jacangelo, 1991). Typically MF membranes have a pore-size of between 0.1 and 1 um such that all suspended material above this size is rejected. The main advantage of a MF system over UF is the higher flux rates at which they are capable of operating and/or the lower operating pressures (0.2 to 2.0 bar). However, MF is generally more susceptible to fouling.

2.3.5 Development of MF and UF in the Water Industry

The use of UF and MF membrane technologies for the production of drinking water has been increasing since the mid 1980's. This is largely due to the need to provide a consistent drinking water quality independent of raw water conditions. Conventional technologies such as sedimentation and filtration, as discussed earlier, produce an effluent whose quality is dependent on that of the incoming water, as well as being

sensitive to the operating conditions of the process, such as chemical dose and hydraulics. The determining factor for treated water quality from a MF or UF membrane is the maximum pore size of the membrane. Variations in raw water quality will affect the throughput and some operating conditions, but not the product quality.

Results from a questionnaire have indicated the growth in the application of MF and UF from 1986 to 1996 (Adham, 1996). The survey showed an increase from 3 plants operating for potable water in 1986 to 74 by 1996. Of these 74 plants 39 used polymeric MF membranes, 34 used polymeric UF and one used a ceramic membrane. The accelerated increase in the use of MF and UF systems for drinking water can be attributed to a number of factors:

- decrease in membrane costs
- development of higher flux membranes
- better understanding of process parameters
- automation potential
- simplicity of operation
- more stringent water quality requirements, and
- emergence of *Cryptosporidium*

2.4 Microfiltration Modes of Operation

There are two modes of operating a microfiltration system for the removal of suspended material. These are crossflow (CF), (Figure 2.6), and dead-end (DE), (Figure 2.7). Either of these two processes may be operated under constant flux or constant pressure conditions (Section 2.9).

The total production flow for any membrane system is simply a product of flux and area:

$$Q_p = J_{tm} * A \qquad (1)$$

where Q_p = system permeate flow rate, l/h

J_{tm} = Transmembrane flux, l/m^2/h

A = Total effective membrane surface area, m^2

The membrane flux is a function of a number of variables including specific qualities of the membrane, feed-water and the operating parameters of the system.

2.4.1 Crossflow Microfiltration

In CF mode the permeate flux is dependent on three factors:

1. membrane properties – pore size, porosity
2. hydrodynamic conditions on the feed side – turbulence, CF velocity
3. rate of permeation required – flux

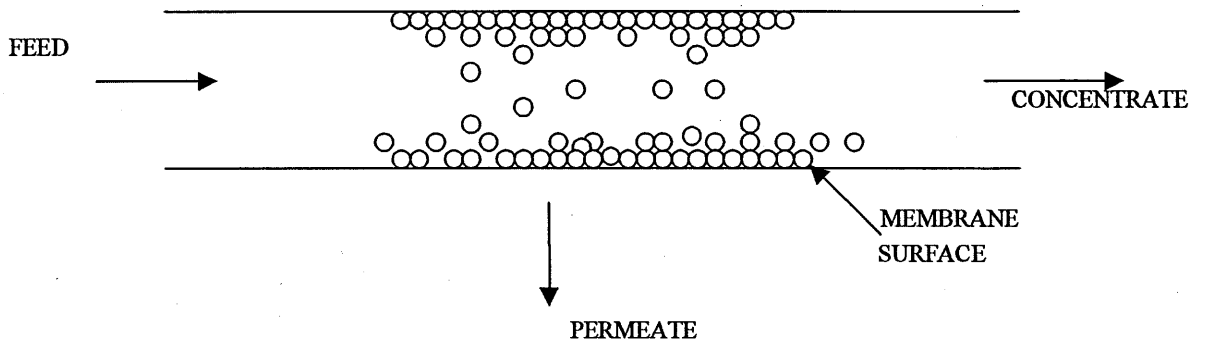

Figure 2.6 Crossflow filtration

In CF mode (Figure 2.6) the rate of conversion of feed water to permeate is governed by the quality of the feed and the rate at which permeate is withdrawn from the system. As permeate is withdrawn the particle concentration in the concentrate stream increases and consequently the flow decreases as a cake is formed at the membrane surface. An equilibrium is reached when the shear forces at the cake/solution interface balance the non-adhesive force between the cake, normally referred to as the "dynamic layer", and the membrane.

The average transmembrane pressure (TMP) for crossflow systems is calculated as follows:

$$p_{tm} = \frac{p_i + p_o - p_p}{2} \qquad (2)$$

p_{tm} = TMP, bar

p_i = Inlet pressure, bar

p_o = Retentate outlet pressure, bar

p_p = Mean permeate pressure, bar

The relationship between the pure water permeate flux (the flow per unit area per unit time) and the Hagen-Poiseuille Law then defines pressure. The majority of waters from which potable water is derived contain varying degrees of suspended material. This suspended material causes an increase in pressure or a reduction in flux due to the formation of the dynamic layer at the surface of the membrane. The permeate flux in a system which contains suspended solids is thus given by:

$$J = k \ln\left(\frac{C_d}{C_r}\right) \qquad (3)$$

where J is the permeate flux in m/s, C_d is the cake concentration, C_r is the concentration in the retentate and k is the mass transfer coefficient in m/s (D/δ - the ratio of the diffusion coefficient to the hydrodynamic boundary layer thickness).

The flux in CF systems can also be expressed in terms of the total resistance to flow, taking into account the resistance due to the membrane, the cake layer and the boundary layer:

$$J = \frac{\Delta p}{\left(R_m + R_f + R_g + R_{bl}\right)} \qquad (4)$$

where R_m the membrane resistance, R_f the fouling layer resistance, R_g the gel layer resistance and R_{bl} the boundary layer resistance, all parameters being expressed in units of pressure per unit flux.

2.4.2 Dead-end Microfiltration (DEMF)

DEMF represents the most established, more simple and most energy efficient (with respect to the operating cycle) form of operation of MF (Figure 2.7). On the other hand, DE operation has implications regarding backflushing and/or cleaning requirements.

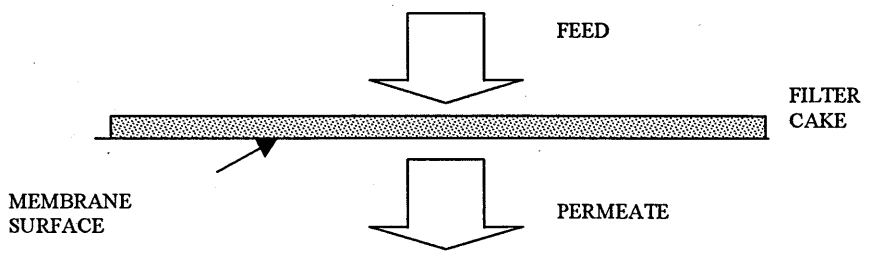

Figure 2.7 Dead-end filtration

In DE all the feed is passed through the membrane such that either the flux drops with time or the pressure increases with time if operated at a constant flux.

For dead-end systems the average TMP is given by:

$$p_{tm} = p_i + p_o \qquad (5)$$

During operation the increase in pressure (or decrease in flux) results from the increasing depth of the cake layer formed on the surface of the membrane. The specific resistance of the cake (i.e. the resistance per unit depth) is determined by the nature of particles in the feed water, specifically their size, shape and compressibility.

When the cake layer reaches a certain thickness, continued operation is no longer viable. In small-scale systems of low total suspended solids (TSS), such as boiler feeds water, the filter itself may be replaced. In large-scale systems the formation of the cake layer is controlled by periodically reversing the flow (backflushing) through the system. The backflushing removes the cake from the surface of the membrane and transports it out of the membrane system.

The efficiency of the backflush is a key component in the operation of continuous large-scale systems. The interval between backflushes is usually determined by pilot-scale tests and usually decreases with increasing feed water TSS. Inadequate backflushing can lead to an accumulation of solids within the membrane and a more rapid increase in driving pressure or a decline in the system production. Poor backflushing necessitates the relatively expensive process of chemical cleaning, which will be discussed later.

2.5 Cake Filtration Theory

2.5.1 Fundamental Cake Filtration

During microfiltration of a fluid containing particles greater than the average pore size of the membrane a cake layer of rejected particles forms on the membrane surface (Figure 2.7). The pressure-driven permeate flux through this cake layer can be derived from Darcy's law assuming total rejection of all suspended particles by the membrane:

$$J = \frac{1}{A}\frac{dV}{dt} = \frac{\Delta p}{\eta_0 (R_m + R_c)} \qquad (6)$$

where J the permeate or volumetric flux, V is the total volume of permeate A the membrane area, t the filtration time, Δp the pressure drop imposed across the cake and membrane, η_0 the viscosity of the suspending fluid, R_m the membrane resistance (which can increase with time due to membrane fouling and compaction), and R_c the cake resistance (which can increase with time due to cake build up and compression). In order to obtain values for both the membrane and cake resistance semi-empirical formulas can be used to estimate these parameters.

2.5.2 Cake Resistance

The specific resistance of an incompressible cake, $\hat{R}_c$, where

$$\hat{R}_c = \frac{R_c}{\delta_c} \tag{7}$$

is given by the Carmen-Kozeny equation (1938):

$$\hat{R}_c = \frac{180(1-\varepsilon_c)^2}{d_p{}^2 \varepsilon_c^3} \tag{8}$$

where, ε_c is the porosity of the cake and d_p the diameter of the particles deposited. The void fraction of a randomly packed cake is conventionally estimated to be 0.4 (Grace, 1953) but has more recently been shown to be between 0.6 and 0.7 depending on the pressure at which the cake is formed (Holdich, 1996).

Many cake materials, such as flocculated clays and microbial cells, are highly compressible. Compressible cakes exhibit a decrease in void volume and an increase in the specific resistance as the compressive pressure is increased (Porter, 1977). The effects of cake compressibility can be estimated by assuming that the specific cake resistance is a power law function of the imposed pressure drop (Belter *et al*, 1988):

$$R_c' = \alpha(\Delta p)^n \qquad (9)$$

where α is a constant related primarily to the size and shape of the particles forming the cake, and n is the cake compressibility, which varies from zero for an incompressible cake to a value near infinity for a highly compressible cake. These parameters can only be determined empirically. For cakes formed on the surface of a hollow fibre membrane, the resistance can be defined as (Shankararaman, 1998):

$$\hat{R}_c = R_c' \rho \phi_c r_0 \ln\left(\frac{r_0 + \delta_c}{r_0}\right) \qquad (10)$$

where ϕ_c, is the volume fraction of solids forming the cake, r_0 is the radius of the hollow fibre.

Assumptions made in Equation (10) are that the cake compression depends on the pressure drop across the combined membrane and cake layers rather than the cake alone. Also, the porosity and specific cake resistance vary throughout the cake height.

2.6 Operation of Dead-End Microfilters

From Equations (6) and (7):

$$J = \frac{\Delta p}{\eta_0 \left(R_m + \hat{R}_c \delta_c \right)} \tag{11}$$

This expression requires the cake layer thickness $\delta_c(t)$ to be known. This may be determined with the aid of a particle mass balance at the edge of the growing cake layer:

$$\left(J + \frac{d\delta_c}{dt} \right) \phi_s = \phi_c \frac{d\delta_c}{dt} \tag{12}$$

where $\phi_s = 1-\varepsilon_s$, is the solids volume fraction in the suspension being filtered, and, $\phi_c = 1 - \varepsilon_c$, is the solids volume fraction in the cake, just below its top surface. The left-hand side of Equation (12) represents the flux of particles into the surface of the cake, and takes into account that this flux is due to the relative motion of the downward flow of suspension and the upward growth of the cake. Back diffusion of fine particles is ignored (Doshi and Trettin, 1981), which is a reasonable assumption. The right-hand side of Equation (12) represents the build-up of particles in the cake. Combining Equations (11) and (12) yields a general equation for the cake layer thickness, the solution of which depends upon the operating conditions:

$$\frac{d\delta_c}{dt} = \frac{\phi_s J}{\phi_c - \phi_s} = \frac{\phi_s \Delta p}{(\phi_c - \phi_s) \eta_0 \left(R_m + \hat{R}_c \delta_c \right)} \tag{13}$$

2.6.1 Constant Flux Conditions

If a positive-displacement pump is used, then the permeate flux through the filter remains constant at its initial value, $J = J_0$. The total volume of permeate V then increases linearly with time:

$$V(t) = AJ_0 t \tag{14}$$

The thickness of an incompressible cake is given by:

$$\delta_c t = \frac{\phi_s J_0}{\phi_c - \phi_s} t \tag{15}$$

To maintain the constant permeate flux, the pressure drop must increase with time, from Equation (14). This linear increase is given by:

$$\Delta p(t) = J_0 \eta_0 \left(R_m + \frac{\hat{R}_c \phi_s J_0}{\phi_c - \phi_s} t \right) \tag{16}$$

For compressible cakes, the analysis is more complicated in that the increase in pressure drop with time causes changes in the cake porosity and in the specific cake resistance, in accordance with Equation (9).

2.6.2 Constant Pressure Drop Operation

Dead-end batch filtration is often carried out with a constant imposed pressure drop. Under such conditions the total permeate volume per unit membrane area, *V(t)/A*, is defined by:

$$\left(\frac{A}{V}\right)t = \frac{\eta_o \hat{R}_c \phi_s}{2(\phi_c - \phi_s)\Delta p}\left(\frac{V}{A}\right) + \frac{\eta_0 R_m}{\Delta p} \qquad (17)$$

Provided R_c is independent of the thickness (i.e. an incompressible cake is formed) and the membrane does not suffer pore blockage, a plot of *At/V* versus *V/A* yields an intercept of $\eta_0 R_m/\Delta p$ and a slope of $\eta_0 \hat{R}_c \phi_s / [2(\phi_c - \phi_s)\Delta p]$ (Figure 2.8). The specific cake resistance is contained in the slope whilst the intercept contains the membrane resistance.

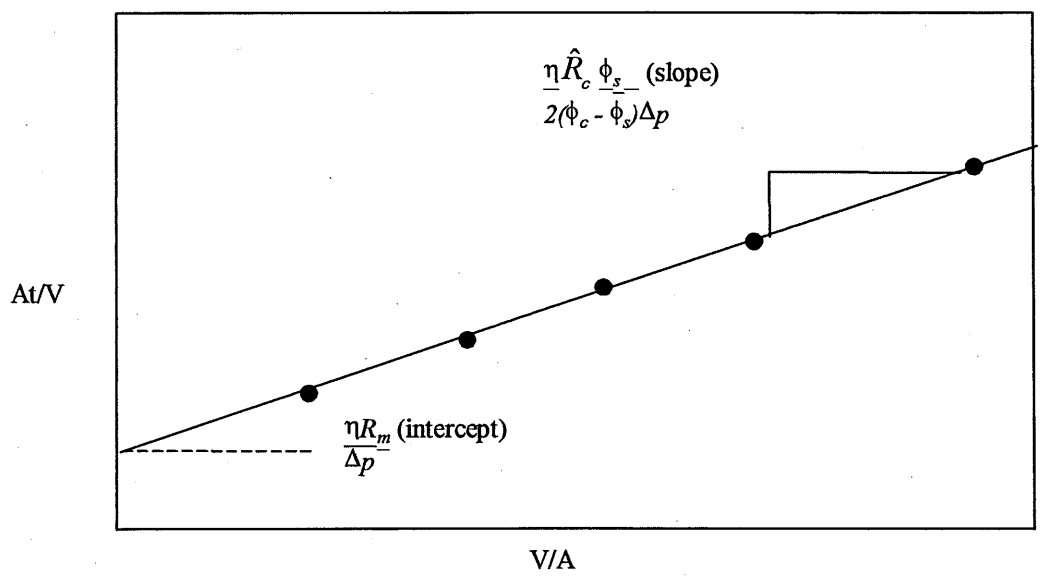

Figure 2.8 Example of a graph used to find the membrane resistance and the specific cake resistance.

2.7 Membrane Fouling

For UF and MF membranes the permeate flux through a membrane defined by an effective pore-size of radius r is given by:

$$J = \frac{fr^2 \Delta p}{8\mu\theta\delta_m} \qquad (18)$$

where f is the friction factor of the open pore area on the membrane surface, θ is the pore tortuosity, and δ_m is the effective thickness of the membrane.

Equation (18) predicts that permeate flux decrease can be countered by increasing Δp. Also, with all other factors being equal a membrane with a larger effective pore radius (or higher MWCO) should have a greater permeate flux.

The accumulation of materials within the membrane e.g. by adsorption to the pore walls or blockage of the pores can result in an increase in R_m over time. Flux decline or TMP increase is produced by both material deposition within the membrane and their accumulation at the surface (as discussed in previous sections). The presence of dissolved and colloidal materials in the feed water can lead to a reduction in the effective pore-size of the membrane over time caused by the adsorption of material on the internal walls of the pores, resulting in a constriction of the pore. Another mechanism for such a reduction in available pore area is pore blocking or the occlusion of pores by solids (see Section 2.7.1)

2.7.1 Pore blocking

The standard pore-blocking model is shown in Equation (19):

$$\frac{t}{V_p} = \frac{1}{Q_0} + \frac{k_s t}{2} \qquad (19)$$

where V_p is the volume of permeate passed at time t, t is the elapsed filtration time, Q_0 is the initial permeate flowrate and k_s the filtration constant:

$$k_s = \frac{2\phi_c}{\delta_m A_0} \qquad (20)$$

where ϕ_c is the volume of solid particles deposited per unit volume of permeate flow and A_0 is the initial available open pore area of the membrane. When the standard pore-blocking model is applied the plot of t/V_p against t should be linear with the intercept equal to $1/Q_0$ and the slope $k_s t/2$.

Pore blocking is caused by the entry into a pore of material either at or near the size of the pore. Two effects may then take place: occlusion takes place when particles plug pores internally; pore narrowing takes place when particles become attached to the wall of the pore. Pore blocking increases with particle size up to a point where the fouling material is greater than the size of the pore and the probability of these larger particles being responsible for pore blocking reduces (Chang *et al*, 1996). These larger particles form a cake at the surface of the membrane.

The formation of a cake on the membrane surface may enhance the removal of smaller particles penetrating the cake by interception or Brownian motion. Cake formation can therefore afford some protection to the membrane from pore blocking. By altering the particle size distribution in the feed stream in order to affect a shift from smaller, pore blocking particles to larger particles that will preferentially form a protective cake the performance of the membrane can be enhanced.

The effect of particle size on permeate flux on a rotary tubular membrane with a pore-size range of 1.9 to 8.0μm and an average pore diameter of 3.8μm operating under constant pressure has been assessed (Ben Aim *et al,* 1993). This work demonstrated the greatest effect on flux decline to be from large particles (4.2μm) compared to the finest particles (2.5μm). This indicated that the smaller particles in this system to be less well retained by this membrane than the larger particles, reducing fouling and so diminishing the flux decline. A permporometer, used to determine the changes in pore size resulting from filtration, revealed the pore diameter to decrease with fouling along with the pore-size distribution. However, the largest pore size was not modified and the permeability of these pores appeared to be unaffected. This indicates that fouling is a function of both the size of particles in the feed and the pore-size distribution of the membrane.

The effects of membrane pore size on fouling have shown that increasing the pore size of MF membranes, from 0.2μm to 5μm, results in an decrease in flux decline when filtering suspensions with a mean particle size of 0.5μm under crossflow conditions (Tarleton and Wakeman, 1993). Results from these authors and those of Ben Aim *et al* (1993) would seem to demonstrate that particulate material at or near the pore size of the membrane causes flux rates to decline more rapidly. Conversely, when the

particulate material was larger than the pore size or significantly smaller the rate of flux decline was less.

A recent study of UF fouling characteristics of clay-organic suspensions demonstrated the complexity of fouling phenomena (Kim, 1996). The system was operated under constant pressure and flux decline measured with time. Combinations of proteins, polysaccharides, humics, fulvics and kaolin were tested. Increasing the concentration of smaller colloids reduced the flux. It was found that different organic combinations had varying effects on the size distribution of kaolin particles and that as the size of kaolin decreased so did the flux.

2.7.2 Hydrophilicity and Hydrophobicity

Membranes in an aqueous environment may have an attractive or repulsive response to water. The bulk material composition of the membrane and its corresponding surface chemistry determine its interaction with water, i.e. its hydrophilicity and hydrophobicity.

Hydrophilic literally means "water-loving" and such materials readily adsorb water. Hydrophobic ("water hating"), materials conversely have little or no tendency to adsorb water and water tends to "bead" on their surfaces forming droplets.

For MF membranes the degree of hydrophilicity influences:

- wettability and applied pressure requirements for liquid (water) flow through the membrane, and
- adhesion characteristics of contaminants to the membrane material, which supplement the retention ability of a given pore, size.

Particles that foul in aqueous media tend to be hydrophobic. Hydrophobic particles tend to cluster or group together to form colloidal particles because this lowers the interfacial free energy (surface tension) due to surface area exposure: spheres of particles are formed because a minimum surface area results in this shape while limiting exposure to the hydrophilic environment. The general tendency will favour particle attachment to any material less hydrophilic than water because less exposure of hydrophobic particles can be achieved by attachment of the particles to a similarly hydrophobic surface. This is typical of the behaviour of colloidal protein, which readily fouls hydrophobic materials such as polypropylene

To ameliorate such fouling demands a surface which displays a preference for binding with water rather than other materials; i.e. hydrophilic.

2.8 Operation of MF Plant

As already stated, MF or UF systems are usually operated either at constant rate (and so constant flux, Section 2.6.1) or declining rate (i.e. constant pressure, Section 2.6.2)

In order to control either the increase in TMP or loss of production, there are three methods that may be employed to remove fouling material:

- Backwashing or backflushing
- Chemical cleaning
- Pre-treatment

2.8.1 Backflushing

Backwashing of membrane systems is a relatively short cycle operation when compared to the backwashing of sand filters: about 10 to 60 minutes compared with 12 to 60 hours for sand filters depending on the feed-water quality. This reflects the vastly increased load capacity of the depth filter over the surface filter.

Over a number of backwash cycles a residual amount of fouling material is left on the membrane surface, and consequently there is either a gradual increase in TMP or a loss of production.

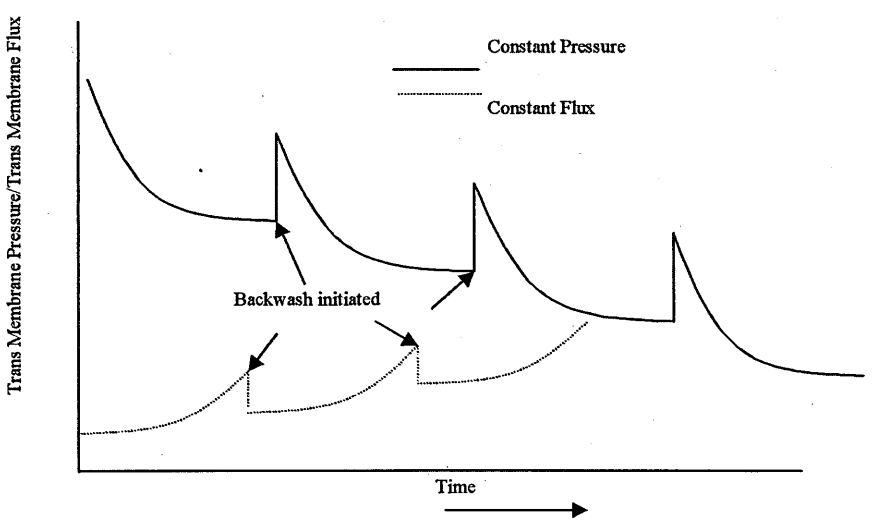

Figure 2.9 Operation of constant pressure and constant flow conditions

Figure 2.9 shows the restoration of performance after backwashing but also shows the gradual loss of performance with time. When the accumulated foulants can no longer be removed from the membrane surface by backwashing, chemical cleaning is required.

The use of backflushing with permeate water to control fouling has some limited potential, particularly in the removal of depth fouling (i.e. particles trapped in the pores of the membrane). A more vigorous in-situ cleaning process based on introducing air at relatively high pressure has been developed for use with a MF polypropylene membrane (Vickers, 1992). This allows the membrane to be used on feeds of higher TSS and more recently the technology has been applied to the treatment of secondary sewage (Van Houtte *et al*, 1998). The air-based backflush is restricted to out-to-in systems.

2.8.2 Chemical Cleaning

There are a range of chemical cleaning agents that can be used to remove residual material retained on the membrane surface. These include acids, bases, oxidants, sequestering agents and surfactants. Effective cleaning is very important in maintaining output of full-scale plants. The material of manufacture and its chemical resistance influence the choice of cleaning chemical, as does the nature of the residual fouling. Many fouling studies have made use of analogues, rather than real waters. Optimum cleaning condition experiments on a range of UF membranes have been undertaken using streaming potential and Fourier Transform InfraRed (FTIR) analysis as an alternative to assessing effectiveness by means of flux restoration (Nystrom, 1996, 1997). Sodium hydroxide was found to be the most effective cleaning agent yielding a

flux recovery of 95% for membranes fouled with BSA (Bovine Serum Albumin- a globular proteinacious material with a high fouling propensity). The major factors influencing the success of the chemical cleaning process were identified as temperature, concentration, pressure and whether or not the membrane is hydrophilic (easier to clean) or hydrophobic.

For potable water production the Drinking Water Inspectorate (DWI) has set regulations that control the use of chemicals and materials used for the production of drinking water and which then limits the choice of chemicals available to water producers. Cleaning normally involves backwashing the cleaning chemical into the system and allowing the membrane to soak for a period of time, up to one hour, before rinsing the spent chemical solution out of the system. Final neutralisation of the chemical waste prior to disposal must then be applied.

A dead-end UF system for the treatment of River Seine water has been evaluated (Lahoussine-Turcard, 1990). Very rapid and irreversible fouling was observed such that the flux declined by 30% after one hour of operation. Cleaning the membrane using a surface water wash produced a flux recovery of 5%, whereas a chemical clean with sodium hydroxide produced a flux recovery of 25%. The sodium hydroxide is thought to dissolve organic material, which had adsorbed to the surface of the membrane.

2.8.3 Pre-treatment

The final way of controlling fouling is by applying some form of pre-treatment. A number of pre-treatment methods have been investigated including microstraining,

addition of metal coagulants and powdered activated carbon (PAC). The purpose of applying a pre-treatment is to remove or modify fouling material so as to ameliorate flux decline.

Raw water supplies vary greatly in their physical and chemical nature, and this has a significant influence on the application of MF or UF. For waters abundant in NOM an additional pre-treatment step is likely to be required to enhance NOM removal. However, understanding of fouling and fouling mechanisms has not yet reached a stage where appropriate pre-treatment can be prescribed in accordance with a given measurable water quality determinand. Adoption of pre-treatment technology is very much based on heuristic observations and rules of thumb.

2.8.4 Coagulation as a pre-treatment to MF and UF membranes

The use of coagulation as a pre-treatment for MF and UF may offer some improvements in the efficiency of the membrane system by removing contaminants responsible for fouling e.g. NOM or sub-micron particles. This improved efficiency may manifest itself in a number of forms:

- increased permeate flux
- reduced backflushing
- reduced chemical cleaning

The potential for enhancement of membrane performance by using pre-coagulation will be dependent upon the nature of the fouling material present in the feed water and their

potential for interaction with the membrane. Such a combination of membrane technology with coagulation pre-treatment for the control of fouling is not new. Using a crossflow system with a bentonite feed (500mg/l) coagulated with WAC (PolyAluminium Chloride (PACl) based coagulant) it has been shown that flux can be enhanced by a factor of eight over the coagulant free system value (Ben Aim *et al*, 1988). The flocculation was proposed to have two major effects:

- eliminating the penetration of colloidal material into the pores, and
- modification of the deposit characteristics

An illustration of these mechanisms, by which coagulation prevents or controls fouling, are shown in Figure 2.10:

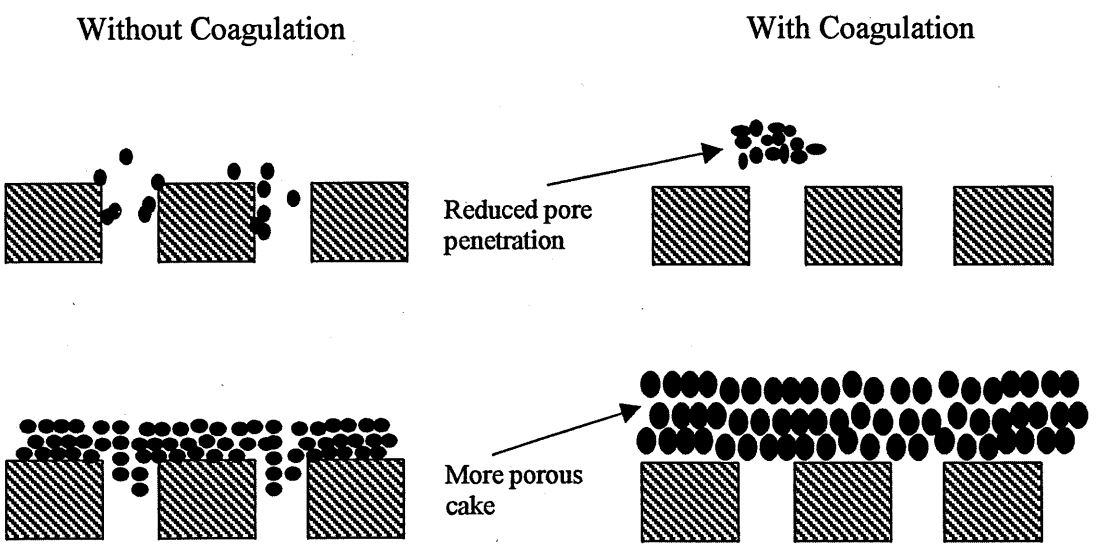

Figure 2.10 Possible mechanisms by which coagulation pre-treatment may enhance membrane performance.

Another observation made by Ben Aim *et al* was that microfiltration does not require growth of large (i.e. >5μm) floc, as would be required in conventional sand filtration process, therefore reducing the amount of flocculation time and/or chemical dose. Also, the authors found that overdosing with coagulant caused a decrease in permeate flux when compared to optimum coagulation conditions. This is probably due to restabilisation resulting in a reduced floc size. However, even when overdosing the performance of the system was enhanced compared to no pre-treatment. The optimum conditions for flux enhancement coincided with the optimum flocculation conditions as determined by conventional jar testing: i.e. the conditions under which the supernatant turbidity and coagulant residual were both minimised.

Table 2.2 gives summary of the relevant operating conditions, membrane materials and key findings of relevant research carried out using coagulation as a pre-treatment to either MF or UF.

There are some common findings presented in Table 2.2, the overriding one being that the pre-treatment of both UF and MF membranes by coagulation can significantly enhance the performance of the process. This enhancement can result in either greater flux rates or reduced fouling, presenting significant benefits for cost effective production of drinking water.

Zeta potential and Surface charge

Particle diameter following flocculation with PACl has been found to increase rapidly between pH 7 and 8, but decrease again once pH values of 8.5 are exceeded. The

maximum particle size and permeability occurred when the zeta potential of the flocculated suspension was near zero (Weisner, 1989).

Similar results have arisen with iron-based coagulant. Large improvements in membrane flux and flux recovery have been achieved using ferric chloride as a coagulant at a dose of 0.6mM as Fe at a pH of 6.5, conditions at which electrophoretic mobility was found to be minimised (Lahoussine-Turcard *et al*, 1990).

The significance of surface charge relates directly to adsorption destabilisation and subsequent flocculation. At zeta potentials at or near zero flocs are at their largest and consequently their propensity to contribute to membrane fouling by blocking pores is reduced. Conversely at more positive and negative potentials floc size is smaller and hence internal membrane pore blocking is more likely (Lahoussine-Turcard *et al*, 1992).

Organic fouling

The main cause of irreversible fouling in UF systems is the adsorption of organic material on the membrane surface (Laine, 1990). By reducing or removing the organic matter by coagulation-flocculation irreversible fouling can be reduced significantly.

The addition of the coagulant PACl has been found to significantly improve the removal of organics, thereby reducing the rate of flux decline by up to 100% (Moulin *et al*, 1991). The normalised flux J/J_0, J_0 being the initial flux and J being the flux at the end of experimentation, increased from 0.25 without coagulation to 0.38 with coagulant and

further increased to 0.55 with coagulant plus chlorine. This second enhancement can be attributed to the oxidative degradation of the fouling organic material by the chlorine.

Cake structure

Coagulation has been found to affect the size and charge of the deposit possibly reducing the degree of adsorption onto the membrane or formation of a cake more easily removed by backflushing (Laine, 1990). Also, coagulation reduced the specific resistance of the cake.

Coagulation pre-treatment was not found to significantly enhance fluxes for 100,000 MWCO membranes but did increase the flux recovery following backflushing (Clark, 1991). The nature of the deposit removed was described as a spaghetti or "straw-like" sludge material formed by the compaction of the flocculated material on the inside of the hollow-fibres. The authors stated that in their opinion the cake was easily removed from the surface of the membrane.

Membrane pore-size

Coagulant prevents colloidal particles entering the membrane and also modifies the nature of the deposit on the surface, both of which tend to enhance performance (Moulin *et al*, 1991). The efficacy of the pre-treatment would therefore be expected to be dependent on the membrane pore size, as has been demonstrated in practice.

	Weisner (1989)	Lahoussine-Turcard (1990)	Lahoussine-Turcard (1992)	Clark (1991)	Laine (1990)	Ben-Aim (1988)	Yuasa (1998)	Moulin (1991)
MF or UF	MF	UF	MF	UF	UF	MF	MF	UF
MWCO or pore-size	0.2μm	1,000 Dalton	0.2μm	10,000 Dalton	100,000 Dalton	0.2μm	0.2μm	50,000 Dalton
Membrane Material	Polycarbonate	Polysulphone	Cellulose Acetate	Polysulphone		Cellulose Acetate	Polypropylene	Polysulphone
Configuration	Disk	Hollow-Fibre	Disk	Hollow-Fibre	Disk	Disk	Hollow-Fibre	Hollow-Fibre
Total Surface Area (m^2)	1.7×10^{-3}	6.2×10^{-3}	1.7×10^{-3}	Not given	Not given	1.7×10^{-3}	40	12.5
Operational Mode	Constant Pressure	Constant Pressure	Not given	Constant Pressure	Constant Pressure	Constant Pressure – CF	Constant Flow	Constant Pressure –CF
Filtration Flux (ms^{-1})	1.38×10^{-6} to 1.38×10^{-5}	1.33×10^{-5} to 4.67×10^{-5}	Not given	Not given	Not given	2.78 to 36.1 $\times 10^{-5}$	1.74 to 2.9 $\times 10^{-5}$	5.56×10^{-5}
Filtration Pressure (kPa)	100	50	Not given	100	275	122.1	20 to 100	70
Specific Flux (ms^{-1}/Pa)	1.38 to 13.8 $\times 10^{-11}$	2.66 to 93.4 $\times 10^{-11}$	Not given	Not given	Not given	2.28 to 29,6 $\times 10^{-10}$	1.5 to 12,5 $\times 10^{-10}$	7.94×10^{-10}
pre-treatment	Coagulation – PACl	Coagulation – PACl or $FeCl_3$	Coagulation – PACl	Coagulation – Aluminium	Coagulation-PACl	Coagulation – PACl	Coagulation – PACl	Coagulation - PACl
Coagulant Concentration (mM)	0.25	0.21 to 1,25 (Al) 0.63 (Fe)	0.1 to 0.32	Not given	0.45	0 to 3	0 to 0.11	0 to 0.9
Water Type	Analogue	River	Analogue	Lake	Lake	Analogue	River	River
Key Finding	Controlling coagulation pH and concentration affects permeability of deposited cake.	Aluminium coagulant reduces rate of flux decline. Largest improvements for conditions of lowest zeta potential	Coagulation conditions at or near zeta potentials of zero produce largest flocs, so reducing their propensity to block pores	Recovery of flux after backwash increased	Coagulation reduces specific resistance (R_c) of deposited cake.	At optimum flocculant dose from jar-tests, permeate flux found to increase by factor of eight.	Pre-treatment with coagulant increases operating flux by factor of 1.67.	Addition of a coagulant reduces rate of flux decline by up to 100%.

Table 2.2. Summary of operating conditions and membrane type for relevant research on coagulation and MF/UF

Thirty-five different membrane systems (22 MF and 12 UF) were evaluated for their ability to treat river water (Kunikane, 1995). The membranes tested were both organic and inorganic in nature with a range of configurations (hollow-fibre, tubular, multitude, plate and frame and bag). Each plant had a capacity of $30m^3$/day and received water without pre-treatment and with a PACl coagulated feed. It was found that the net water production of both the MF and UF systems have similar ranges, 45 to 308 m^3/m^2 for MF and 63 to 315 m^3/m^2 for UF. In order to maintain flux in MF systems pre-treatment with PACl was found to be necessary. This was not the case for UF, due to the smaller pore sizes involved. The authors also reported that dead-end filtration was more energy efficient than crossflow operation.

2.8.5 Other Pre-treatment Options

Both MF and UF systems have been combined with a range of pre-treatment conditions including coagulation/PAC/MF, UF/ O_3/GAC, coagulation/O_3/PAC/MF and prefiltration/O_3/PAC/UF (Magara *et al*, 1998). All combinations of these processes effectively removed NOM and consequently reduced THMFP. It was found that that using the membrane system prior the O_3/GAC reduced THMFP due to the effective removal of particulate organic matter by the membrane.

UF with a MWCO of 100,000 was combined with PAC under crossflow conditions (Jacangelo, 1995). The primary objective of this study was to remove NOM and consequently control THMFP. Previous work had shown that the raw water in this study did not show significant fouling over extended periods of operation (>330h). Thus any short-term increase in TMP could be attributed to the addition of PAC. The

addition of PAC was found not to significantly increase TMP even at concentrations up to 200mg/l. Moreover, there appeared to be a decrease in TMP with increasing concentrations of PAC. This is probably due to removal of significant amounts of organic material which would normally cause fouling of the membrane. The effect of pre-treating two different UF systems with PAC to treat river water has been evaluated (Yuasa, 1998). In comparing the product water quality via pre-coagulation and pre-treatment with PAC, it was revealed that both processes removed turbidity, NOM and metals. However, the use of PAC as a pre-treatment had the added advantage of removing dissolved organic micropollutants such as pesticides. A contrasting observation was found whereby the addition of PAC prior to a UF membrane, with a MWCO of 100,000, yielded adverse effects (Lin *et al*, 1999). The PAC was found to be ineffective at removing certain molecular weight fractions which were identified as having the greatest effect on flux decline, i.e. MW >17,000. However, PAC when added to deionised water and then filtered was found not to affect flux decline, in fact permeate production was better than with deionised water alone. In contrast, combinations of PAC and humic substances exhibited significant flux decline. The observed flux decline was attributed to humic substances deposited on the surface of the membrane that were not removed by PAC addition.

An alternative method for controlling fouling involves a compromise between flux and pressure development (Field *et al*, 1995), and concerns the concept of "critical flux". The critical flux hypothesis for MF is that on start-up there exists a flux value below which the usual transient flux decline does not occur. This critical flux value is dependent on the hydrodynamics of the system as well as other variables such as feed-water quality and membrane pore-size. The consequences of operating below

the critical flux are an improved flux recovery after chemical cleaning and increased membrane life. However, the capital costs of large systems designed at low fluxes are high and may be prohibitive. Modification of the fouling material prior to filtration by coagulant dosing may increase the value of the critical flux and hence the long-term system performance. However, such pre-treatment increases the chemical demand and waste generated by the process.

3.0 MATERIALS AND METHODS

3.1 Materials

3.1.1 Membrane Module

A hydrophilic polyethersulphone hollow-fibre Optimem™ membrane supplied by USF Acumem, Gorsey Lane, Widnes was used throughout. The membrane pore diameter had a mean value of 0.1μm and a maximum value of 0.2μm. The membrane module contained approximately 3,720 fibres with each fibre having an internal diameter of 0.8mm, an external diameter of 1.5mm, and a length of 0.8m. The total filtration area contained within the module was 9.6m^2. The direction of flow through the fibres was from the inside to the outside, and the module was designed to operate in dead-end mode.

3.1.2 Membrane Pilot Plant

The microfiltration pilot plant used had a maximum throughput of 70,000 l/d. It comprised a 500 litre raw water holding tank, a booster pump, a 200μm strainer, two in line mixers and a permeate holding tank all in series (Figure 3.1). The strainer was set at 200μm so as to prevent blockage of the hollow-fibres by larger particulate material and also afford some protection to the membrane. The flowrate was set so as to achieve a constant flux rate of 110 lmh. Operation was full-flow ("dead-end") with regular backflushing and periodic chemical cleaning.

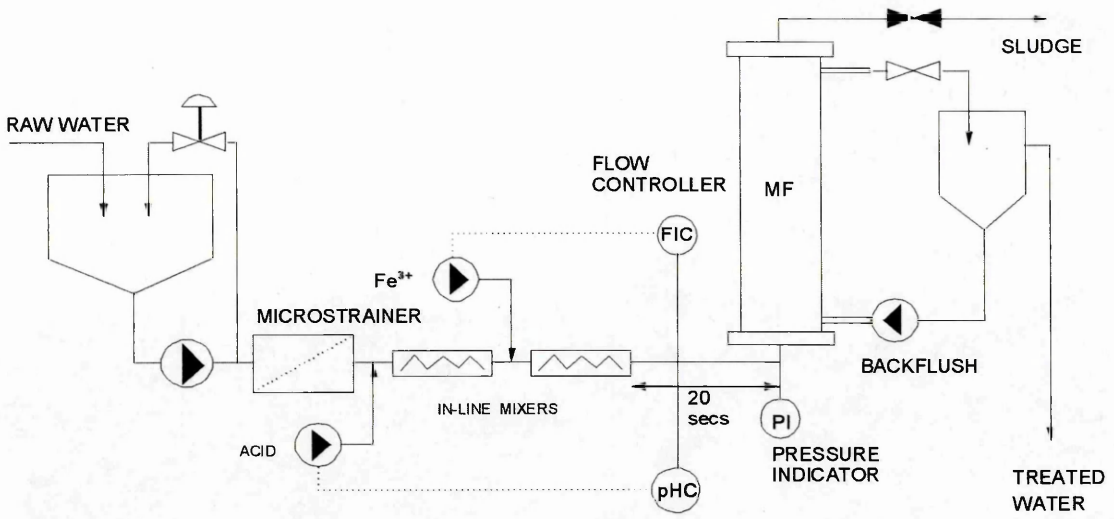

Figure 3.1 Process schematic for NOM removal by microfiltration with pre-coagulation.

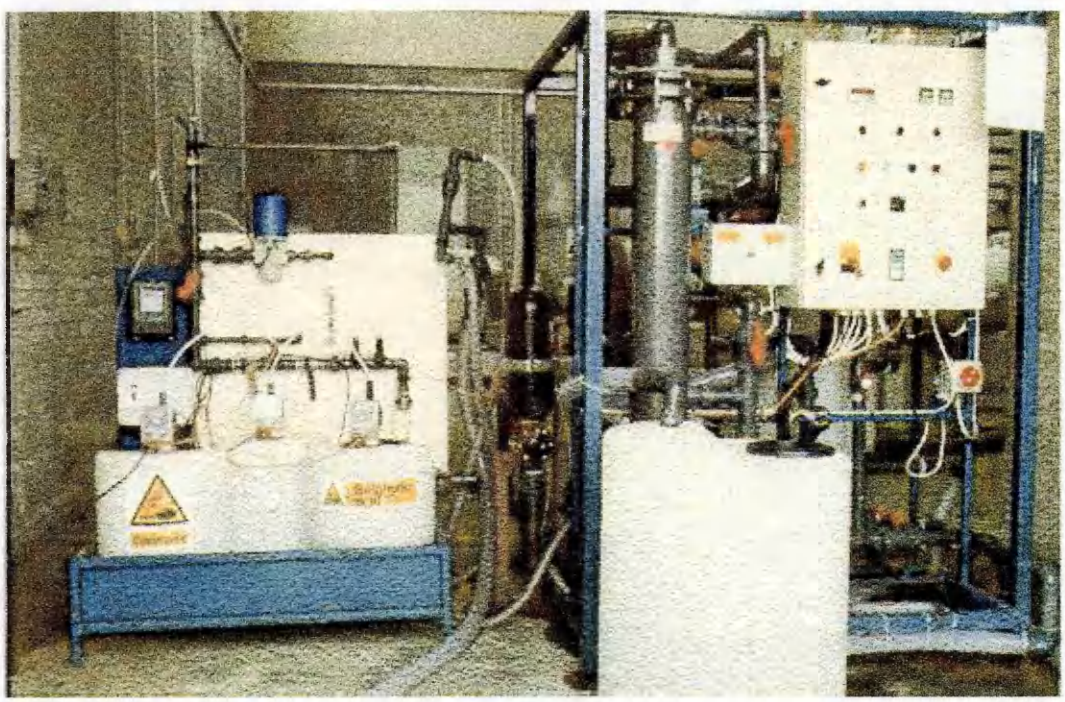

Figure 3.2 Membrane microfiltration pilot plant as built

Table 3.1. List of pilot plant equipment

Item	Purpose and Specification	Manufacturer
Raw water pump	Pumping water to pilot plant over operating flow and pressure rang	Lowara
Raw water strainer	Protection of membrane from large particulate material, rated at 200μm	SPINCLEAN™, Industrial Filter and Purification Systems
Coagulant dosing pump	To add coagulant to raw water	Prominent Gamma 4a
Sulphuric acid dosing pump	To add sulphuric acid to raw water	Prominent Gamma 4a
Two In-line static mixers	To mix added chemicals	Chemineer Kenics 5 element helix flash mixers
Flow controller	Flow proportional control of coagulant chemicals	Endress and Hauser
pH controller	To control pH of coagulation to 5.5	Endress and Hauser CPM 240
Backwash pump	To pump backwash water through the membrane	Lowara
Pressure indicator	To indicate inlet pressure to membrane module	S and M Gauge Co.
Membrane module	$10m^2$ membrane to remove particulate material, rated 0.2μm	US Filter –Optimem

3.1.3 Laboratory Equipment

The following laboratory equipment was used for jar testing, particle monitoring and analysis of water sample:

Stuart Scientific Flocculator, Model No.SW1 (for jar-testing)

Corning 240 pH Meter

HACH Ratio Turbidimeter

HACH DR/4000U Spectrophotometer (for colour and UV absorbance)

Hiac-Royco LV Versacount particle monitor

0.45 μm Sartorious cellulose acetate laboratory membrane filter (for sample filtration)

3.2 Methods

3.2.1 Jar Testing

Optimum coagulant dose and pH conditions were determined through a series of standard jar test experiments. The procedure used was based on a standard WRc procedure (Hall and Hyde, 1992).

Sulphuric acid (0.5M) was used for pH correction and low manganese grade ferric sulphate (0.018M Fe^3, Industrial Alum Ltd, 10%w/w as Fe^{3+}) was used as the coagulant. Six one litre samples of raw water were collected and tested simultaneously with different amounts of chemicals (ferric sulphate and sulphuric

acid). These were added and rapid mixed at 230 rpm for 1 minute, followed by 15 minutes of flocculation at 30 rpm to promote growth of floc material. The samples were then allowed to settle for 15 minutes. The supernatant was slowly withdrawn using a 100ml plastic syringe to avoid disturbance of any settled material and analysed for pH, turbidity and residual iron. In addition, a sample of the supernatant was filtered and analysed for colour at 400nm and UV absorbance at 254 nm, UV absorbance has been identified as a good surrogate for NOM (Owen *et al*, 1993).

3.2.2 Jar Test in Conjunction with Particle Monitoring

The short-term change in particle size during the coagulation process was investigated using conventional jar-test equipment in conjunction with a Hiac-Royco LV Versacount particle monitor.

The particle monitor was set to sample approximately every 2.4 seconds with the sample line inserted in the jar containing 1-litre sample water to be tested. The paddle speed was set to 230rpm and the background raw water particle count established over an initial 30-second period. Sulphuric acid (0.5M) and low manganese ferric sulphate (0.018M Fe^{3+}) were added and the rapid mixing continued for a further 150 seconds whilst the particle count was being measured. The delay time from the jar test equipment to the particle monitor was determined by tracer studies to be 17.5 seconds.

A series of experiments were carried out so as to establish whether the particle counter was recording the precipitation of iron (III) hydroxide or the aggregation of

colloidal and sub-micron particles as a result of charge neutralisation coagulation. These experiments consisted of monitoring the change in particle count with time for the following series of samples:

- Raw water (NOM and particles)
- Raw water filtered through 0.2um filter paper (NOM and particle free)
- De-ionised water filtered through 0.2um filter paper (particle free)

Experiments were carried out at a coagulant dose of 0.036mM, with the pH set to 5.5 and again plots of particle concentration versus time were plotted.

3.2.3 Pilot Plant Trials

The experimental program was developed to determine the feasibility of using MF with pre-coagulation as a process for the removal of NOM, and in particular THM precursors such that the maximum THM formation potential (THMFP) of the treated water was below the PCV of 100µg/l for total THM. Once the feasibility was established, the optimum conditions were investigated, in terms of ferric dose, inlet pressure build up as the run progressed, backflush conditions and the chemical clean regime.

Pilot plant operation comprised an operational cycle and a cleaning cycle. During operation water from the raw water holding tank was passed at constant flow through a 200µm strainer before sulphuric acid was added prior to the first in-line static mixer, the dose being regulated by an in-line pH controller. The coagulant was

injected after the first static mixer and prior to the second with the dosing rate being controlled by a flow sensor. The hold up volume of the system allowed a delay of 20 seconds between coagulant addition and entry into the MF system.

The membrane module was backflushed every 10 minutes with 5% of the permeate flow and then purged with 1% of the feed water flow. Backflushing was achieved by reversing the flow through the membrane, via a separate pump, at a flux of 400 lmh and a pressure of 2.0 bar.

Cleaning was carried out at the end of each 24 hour trial using 1% sulphuric acid to remove residual ferric material followed by a 1% sodium hydroxide clean to remove any organic material which had fouled the membrane. The cleaning process consisted of backflushing the sulphuric acid cleaning solution through the membrane and allowing to soak the membrane for 30 minutes. Following the 30 minute soak the system was purged with the raw water crossflowing across the surface of the membrane and out of the module. The process was then repeated using sodium hydroxide cleaning solution.

The initial TMP was measured after the cleaning cycle by returning the membrane system to permeation at the pre-set flux of 110 lmh. Provided the TMP was found to be acceptable (i.e. less than or equal to 35,000Pa) the next experiment was set up. For residual TMP values 35,000Pa the cleaning cycle was repeated until the system reached the benchmark TMP.

The coagulant dose was varied from 0 to 0.072mM as Fe. With no chemical pre-treatment the system was operated at ambient water conditions (*ca.* pH 7). During coagulation experiments the optimum pH value for NOM removal, as determined in bench scale jar tests, was employed.

The run time for experiment termination was fixed at 24 hours, due to operational constraints of the site where the tests were based. The effectiveness of the chemical cleaning procedure was assessed through the recovery of specific flux (flux per unit TMP) to ensure that subsequent operation was not affected by residual fouling present at the start of a run.

Samples of feed and permeate were taken and analysed by NWW Laboratory Services using accredited methods for the following determinands:

Iron and Manganese (ICP)

Colour (Spectrophtometric)

Turbidity

THMFP[1] (GLC)

pH

[1] This test is a simulation of the potential of any water to form trihalomethanes and consists of chlorination (to excess), pH elevation (>9.0) and storage (7 days), thereby allowing the water to be exposed to the conditions under which THM formation is most enhanced.

4.0 RESULTS AND DISCUSSION

4.1 Jar Tests

Jar tests were carried out over a range of coagulant doses and pH values to determine the optimum operating conditions for conventional treatment, as described earlier. The optimum conditions were determined by analysis of supernatant water quality parameters, which indicate maximum removal of NOM, as measured by UV absorbance at 254 nm and minimum coagulant metal residual after filtration through a 0.45µm laboratory membrane filter. The results are shown in Figures 4.1 and 4.2.

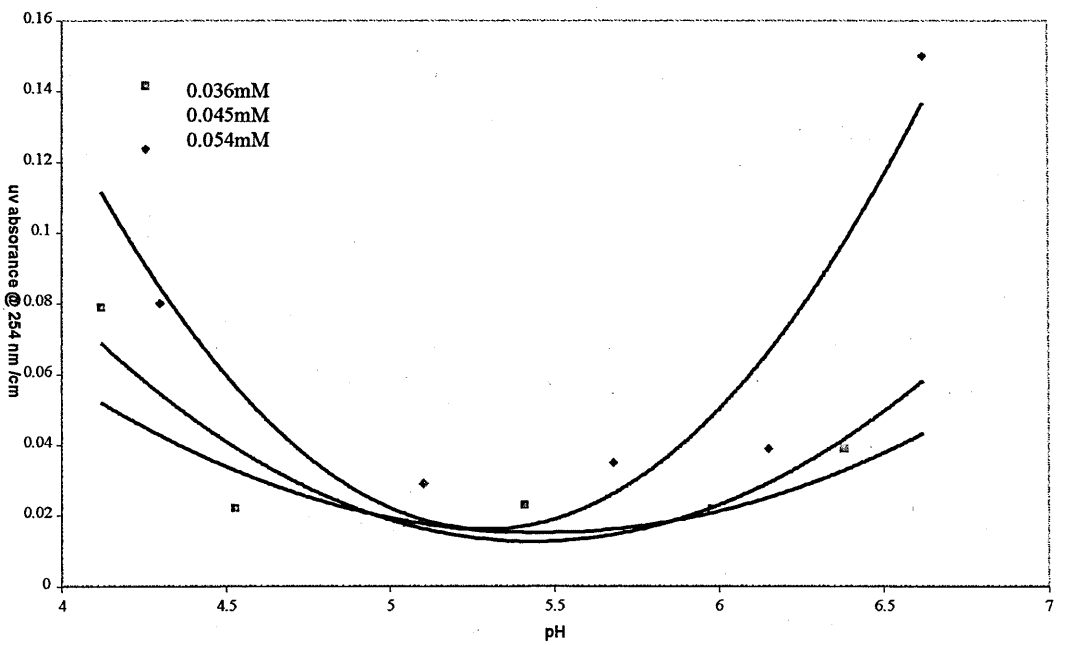

Figure 4.1 Jar Test Results of U.V absorbance at 254 nm vs. pH at different ferric doses.

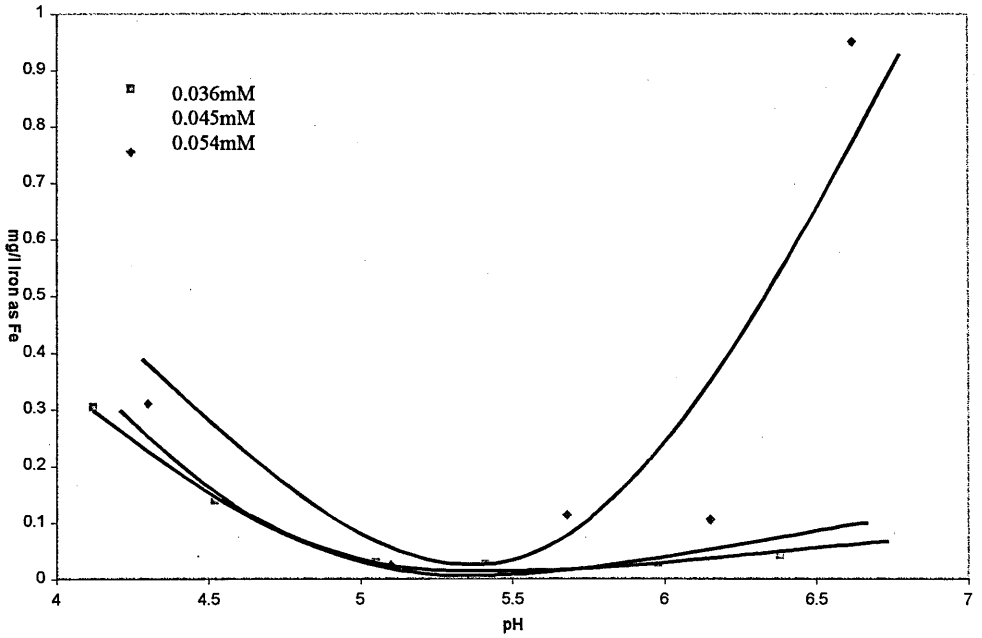

Figure 4.2 Jar-test results of coagulant residual vs. pH at different ferric doses.

Both Figures 4.1 and 4.2 show that over the range of coagulant doses and pH conditions investigated a minimum coagulant residual and UV absorbance occurs at a pH between 5.2 to 5.5. This minimum did not change significantly with coagulant concentration. These conditions are presumed to correspond to the conditions at which the charge neutralisation coagulation mechanism is favoured (Johnson and Amirtharajah, 1983).

4.2 Particle Count Data From Jar Tests

Particle analyses were carried out over a range of coagulant dose and pH values to determine the short-term rate of particle formation, a crucial parameter since the time between coagulant addition and entry into the MF system is only 20 seconds. Figure 4.3 shows the change in the number of 2-5μm particles with time at a range of

coagulant doses at optimum pH conditions (5.2 - 5.3), for NOM removal (Figures 4.1 and 4.2).

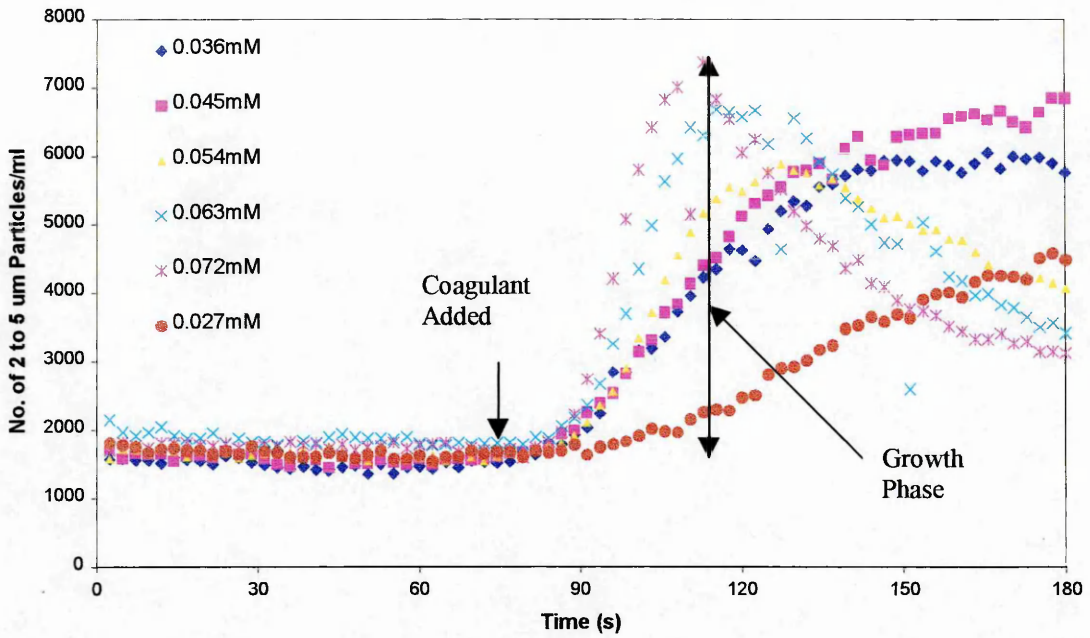

Figure 4.3 Number of 2-5μm particles formed, as a function of time, after the addition of ferric sulphate coagulant, at pH 5.2-5.3, to raw water.

It is clear that the rate of formation of particles increases with coagulant dose according to a sigmoid function with a neo-linear rate of formation in the growth phase when the slope is at a maximum. Similar effects have been seen when a PDA 2000 was used in combination with a jar-test apparatus to monitor Flocculation Index (FI) (Section 2.2.6). The PDA 2000 measures the average transmitted light intensity through a flocculated suspension and the fluctuations in the signal; the ratio of these allows derivation of FI (Gregory and Hiller, 1995). The sigmoid curves obtained by plotting FI vs. time are given by:

$$FI = a + \frac{b}{1 + \exp\left(-\frac{t-c}{d}\right)} \qquad (21)$$

where a, b, c and d are fitting parameters.

The parameter a is the initial value of FI before flocculation, b is the plateau level achieved after sufficient flocculation, c is the time to reach the inflection point of the maximum slopes of the curve and d is a function of the slope at that point. In this case b, c and the maximum slope, s can be used as a measure of the effectiveness of the flocculation process (Figure 4.4). The parameter b should be related to floc size and the greater this value the larger the flocs. The parameter c is a function of the stirring rate and s should be closely linked to the rate of flocculation.

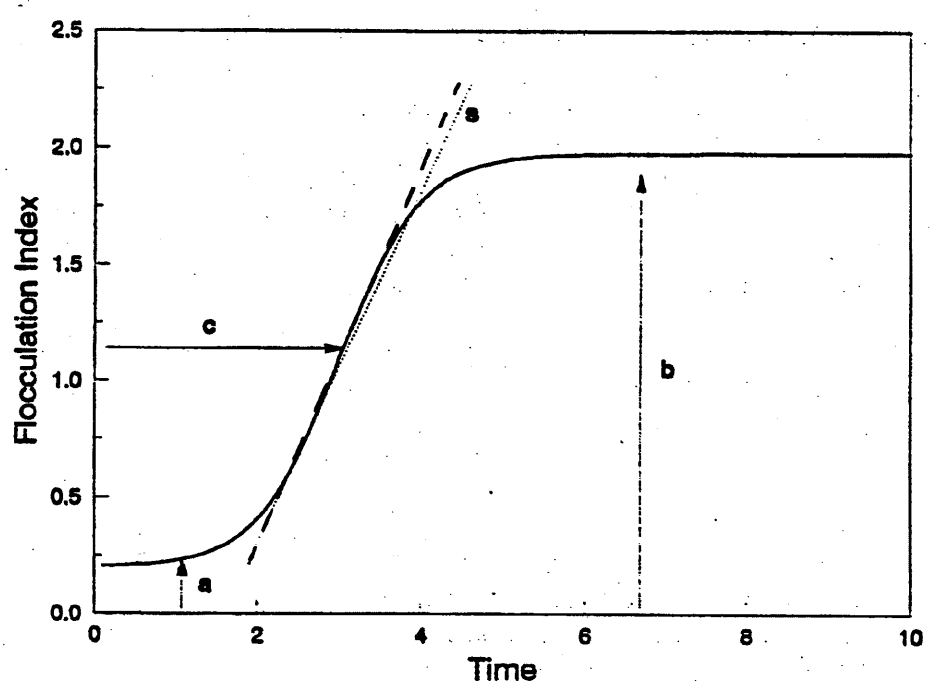

Figure 4.4 General form of sigmoid curve, representing the change in flocculation index with time (Gregory and Hiller, 1995)

By plotting the rate of formation during the period of maximum growth rate, s, in accordance with Gregory and Hiller (1995) for the data presented in Figure 2.5, against coagulant dose a comparison of results can be made (Figure 4.5).

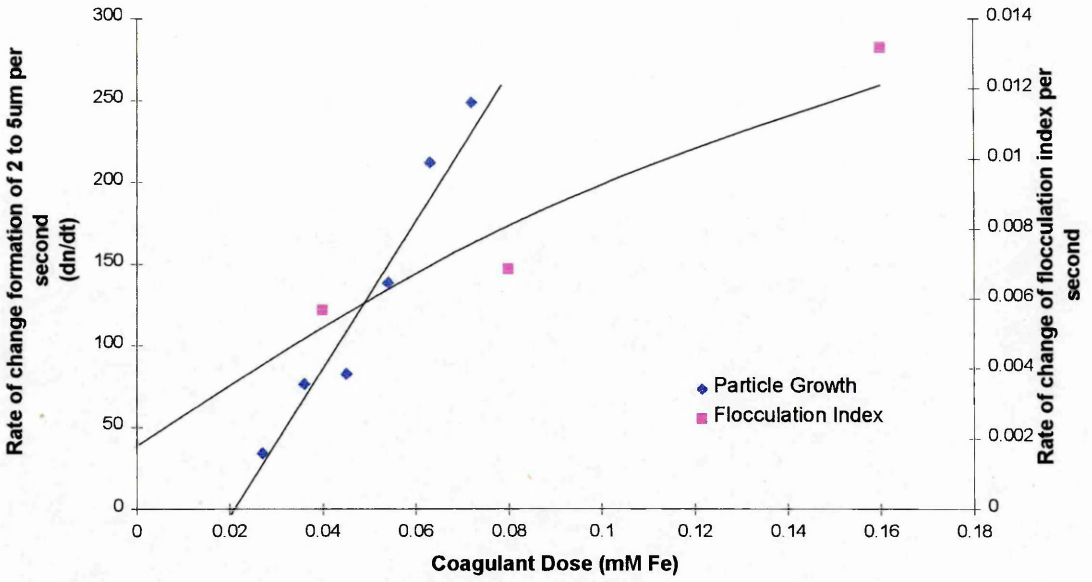

Figure 4.5 Rate of particle formation ($dn_{2\text{-}5\mu m}/dt$) at pH 5.5 and change in flocculation index at pH 7.0 for different coagulant doses.

Figure 4.5 shows that the rate of particle formation and the rate of change in flocculation index are both a function of the coagulant dose under fixed conditions of pH. The plot shows that there appears to be a threshold value below which the addition of coagulant does not cause destabilisation of particles and hence growth. It should be expected that both systems would observe this trend since both rely on growth of particles as a result of addition of a coagulant. However, the Gregory and Hiller data shows a near linear response of floc growth rate (through FI), with a positive displacement at zero coagulant dose. This may be due to the use of kaolin, which can flocculate in the absence of a coagulant.

The pilot plant system was set to operate with a 20 second flocculation time before entry into the membrane module. By measuring the percent "conversion" or formation of particles from onset of the increase in particle count some insight into

the flocculation kinetics can be attained. Figure 4.6 shows a plot of the percentage conversion with time normalised against the maximum number of particles formed, as given in Figure 4.3.

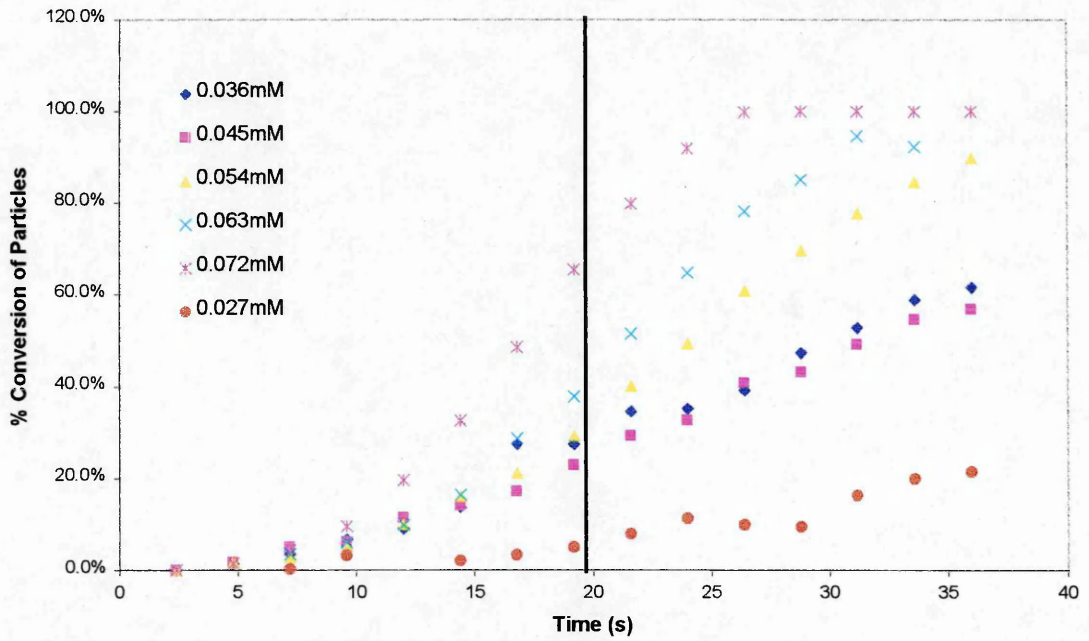

Figure 4.6 % "Conversion" of particles with time

As the coagulant dose increases beyond 0.054mM so does the number of 2 to 5μm particles within the 20 second flocculation time (Figure 4.7).

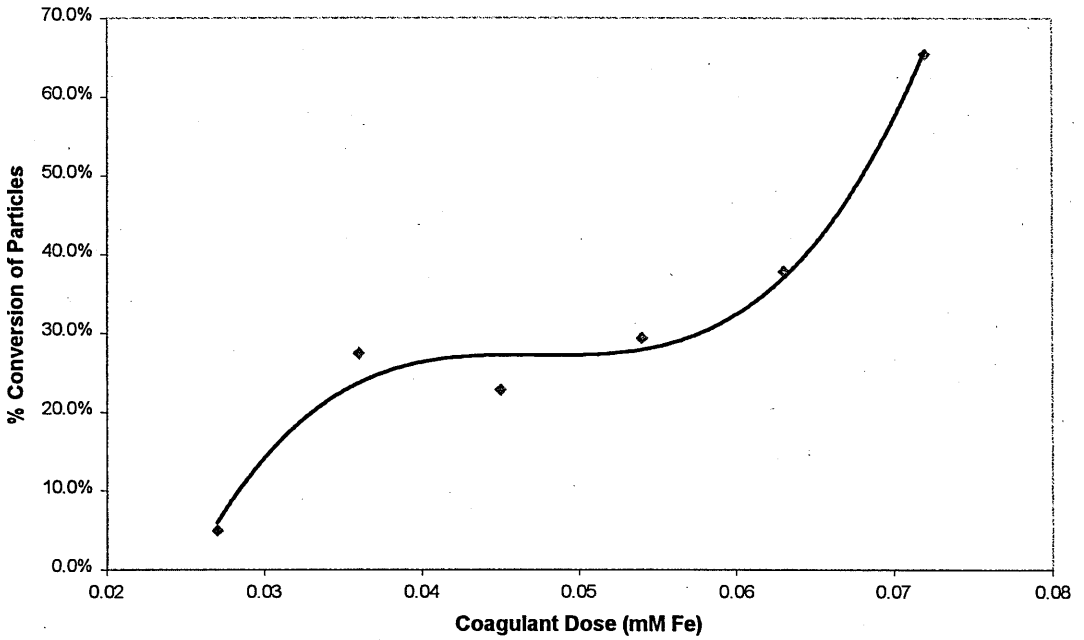

Figure 4.7 % Conversion of particles at various coagulant doses after 20 seconds reaction time.

Figure 4.7 indicates that even at the highest dose of 0.072mM, 100% conversion is not achieved before 20 seconds of reaction time have elapsed. Thus, over the coagulant dose range studied, increasing coagulant dose always results in a greater number of larger particles present in the cake formed at the membrane surface. Thus the average particle size in the deposited material is significantly larger at the higher doses and hence its specific resistance to filtration is lower, as dictated by the Carman-Kozeny equation.

To further elucidate the coagulation mechanism (i.e. adsorption destabilisation vs. sweep) a comparative series of jar-tests was carried out using deionised water and raw water filtered through a 0.2μm filter paper. A coagulant dose of 0.036mM of Fe was used and the same experimental procedure conducted as with previous experiments using the particle counter combined with the jar-tester.

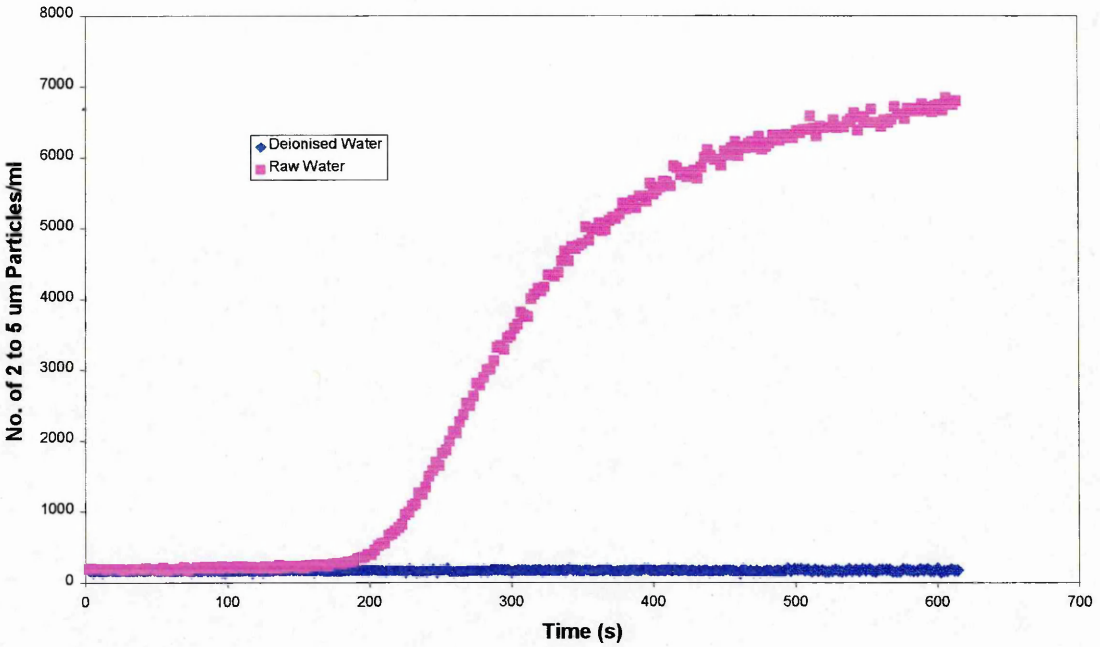

Figure 4.8 Number of 2-5μm particles formed, as a function of time, after the addition of 0.036mM of Fe^{3+} to de-ionised water and raw water, both filtered to 0.2μm

It is clear from Figure 4.8 that there is no measurable increase in the formation of 2 to 5μm particles when deionised water is dosed. If the coagulation mechanism under these conditions involved homogeneous precipitation the particle counter would be expected to record an increase in particles independent of the make-up of the test water, due to precipitation of ferric hydroxide. Conversely, a significant increase in particle count arises from the dosing of raw water is used, for which dissolved and colloidal organic material are present. The reaction of NOM with either monomeric or polymeric ferric hydroxy species is kinetically faster (10^{-4}s to 1s) than the homogeneous precipitation of ferric hydroxide (>1s to several years according to Rebhun and Lurie, 1993). Thus it is the formation of ferric-NOM complexes/precipitates that is being measured by the particle counter in the presence

of NOM in the raw water, which cannot take place in deionised water. The colloidal NOM is removed by charge neutralisation via positively charged hydrolysis products; soluble NOM is removed by the precipitation of iron humates (Randtke, 1998).

4.3 Zeta Potential measurements

Figure 4.9 shows a plot of the zeta potential of the coagulated water at different coagulant doses.

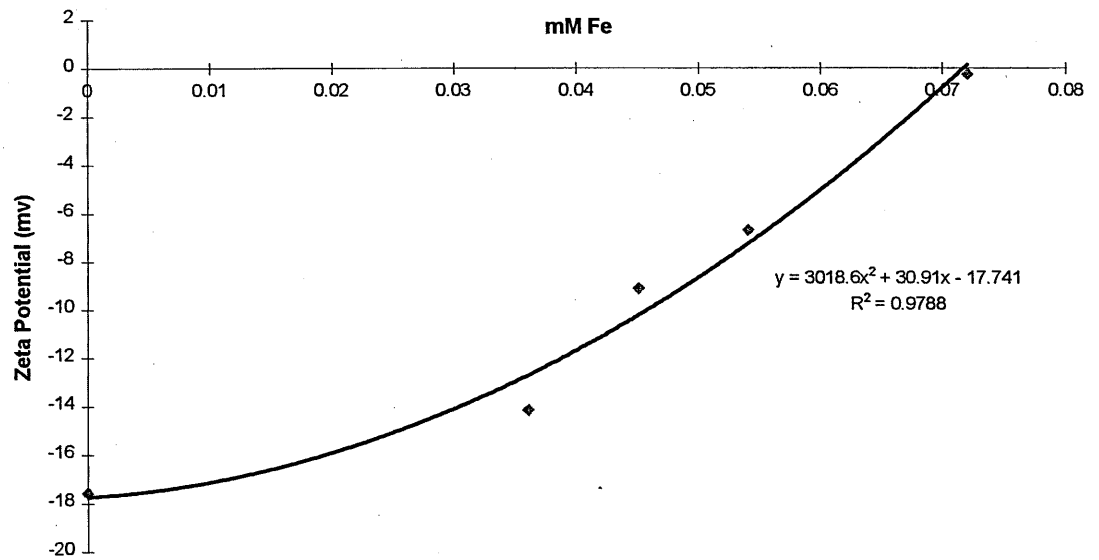

Figure 4.9 Zeta potential at different coagulant doses at pH 5.5, raw water pH 6.7

As the coagulant dose was increased from zero to 0.072mM as Fe, the zeta potential decreased to zero, thus reducing the repulsive forces between particles and so allowing aggregation to occur. The coagulant concentration at the point of zero charge (0.072mM) coincides with the maximum aggregation rate as evidenced in Figure 16. This supports the proposal that over the range studied the coagulant dose increases the average size of particles in the cake, such that the resistance to filtration

decreases. Also, it is likely that there are fewer sub-micron particles present at the higher coagulant doses leading to a decrease in internal fouling by pore blocking (Weisner, 1989, Tarleton and Wakeman, 1993, and Chang *et al*, 1996).

4.4 Pilot Plant Experiments

The MF pilot rig was set up to operate over the range of coagulant doses between 0 and 0.072mM as Fe^{3+} at pH 5.5. The rate of inlet pressure development with time, at a constant flow of 1.1 m^3/h and a backwash interval of 10 minutes and duration of 8 seconds, was recorded (Figure 4.10). In almost all cases the pressure development shows a linear correlation with time, the exception being the zero-coagulant trend.

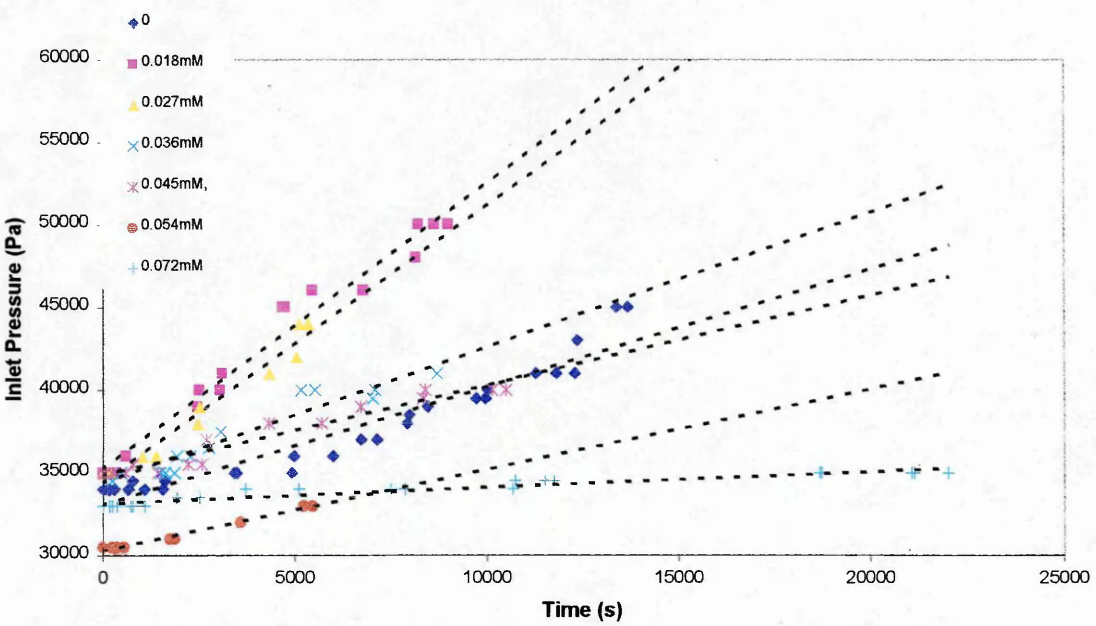

Figure 4.10 Pressure development with time at different coagulant doses.

The performance of the membrane as represented by inlet pressure development is poor in the absence of coagulant. This almost certainly results from pore blocking and surface fouling caused by colloidal organic material. Also, any cake formed is composed of the smallest particles which then present the highest resistance to filtration.

Pre-treatment with ferric coagulant had an initially deleterious effect on performance, as evidenced by the more rapid rate of pressure development *dp/dt* at coagulant concentrations of 0.018mM and 0.027mM (Figure 4.10). This may be due to incomplete aggregation at low doses resulting in particle growth at or near the pore-size of the membrane causing increased internal fouling. Figure 4.5 clearly shows the rate of particle growth to be a function of coagulant dose. At the lower doses the growth rate is slow leading to an increased concentration of smaller particles of approximately the same size as the membrane pores. At low coagulation rates colloidal particles trapped in the pores may aggregate to produce larger particles capable of constricting or blocking the pores (Ben Aim *et al*, 1988 and 1993). These particles are less readily dislodged by the backwash cycle.

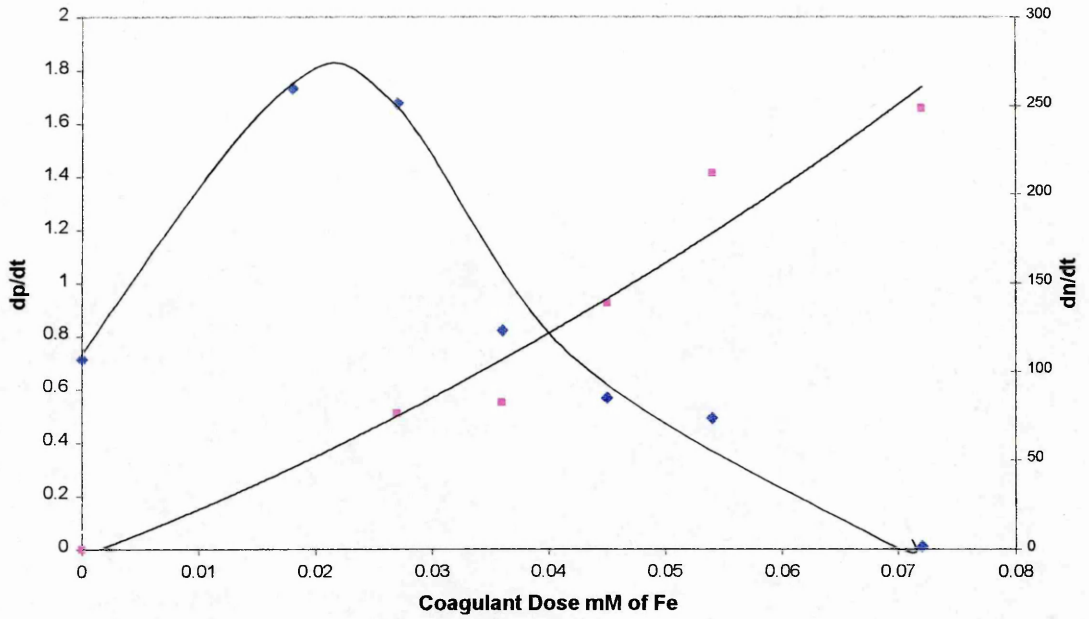

Figure 4.11 Rate of change of pressure development and particle formation with time at different coagulant doses.

Figure 4.11 shows that *dp/dt* initially increases, and this is likely to be due to kinetic limitations of the coagulation process causing aggregation of particles within the pores of the membranes. The maximum *dp/dt* is found to occur at approximately 0.020mM of Fe. Once the coagulant dose is increased beyond 0.020mM of Fe *dp/dt* decreases exponentially with coagulant dose and approaches zero when the concentration of coagulant is 0.072mM of Fe. The near zero value of *dp/dt* corresponds to zero zeta potential (Figure 4.11). It also interesting to note that the measured flocculation rate is correspondingly, as determined by the rate of growth of particles with time (Figure 4.5), is also at a maximum at the point of zero zeta potential.

According to classical filtration theory (Section 2.6.1), a plot of the rate of change of pressure with time yields a slope of:

$$slope = \frac{\hat{R}_c \eta_0 J_0^2}{\phi_c - \phi_s} t \qquad (22)$$

The specific resistance of the cake to filtration ($\hat{R}_c$) is directly proportional to the rate of change of pressure with time over the operational cycle. The pilot plant system used in this work relied on manual reading of measurements of pressure. $\hat{R}_c$ was calculated on the basis of two or more readings over the course of a single operational cycle of 10 minutes, assuming a linear increase of pressure with time.

As already explained (Section 2.6.1), as filtration progresses there is an increase in pressure in order to maintain a constant flux. The use of backflushing reduces this pressure increase but does not eliminate it, as there is always a residual deposit not removed by backwashing. Residual cake resistance values ($\hat{R}_c'$) based on the pressure transients shown in Figure 4.10 are presented in Figure 4.12 along with the operating $\hat{R}_c$ values. From $\hat{R}_c$ the mean particle diameter is determined according to the Carmen-Kozeny equation (Figure 4.13).

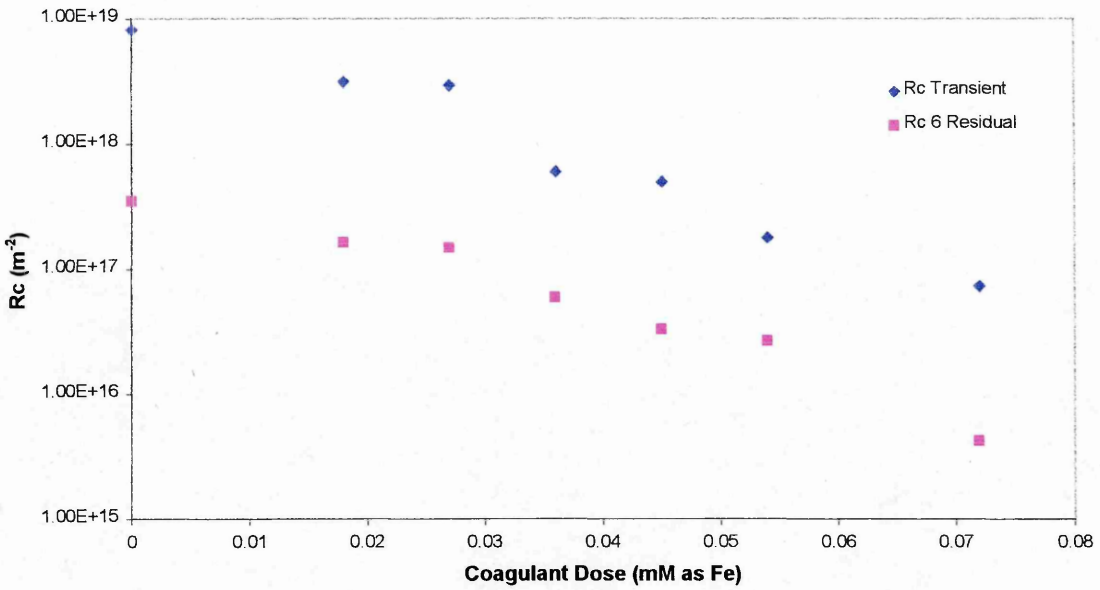

Figure 4.12 $\hat{R}_c$ versus coagulant concentration for the transient and residual ($\hat{R}_c'$) cake

The resistance of the membrane itself (R_m) can be determined from Equation (16) using the mean value of the intercepts from Figure 4.10. R_m is calculated to be 7.3 x10^{11} m^{-2} and this compares to a minimum value of 4.22 x10^{15} for $\hat{R}_c$. Thus, even when operating at the highest coagulant dose with a correspondingly small pressure increase, the resistance of the "cleaned" membrane is apparently four orders of magnitude less than that of the cake of least resistance.

It is apparent that the Carmen-Kozeny equation does not yield representative particle size data, as measured directly by the Hiac-Royco LV Versacount particle monitor (Figure 4.3), the particle size measured being substantially higher. This may be due to the fact that there is a lower limit of 2μm with the particle counter and there may be a significant number of predominant sub 2μm particles present in both the raw and coagulated samples.

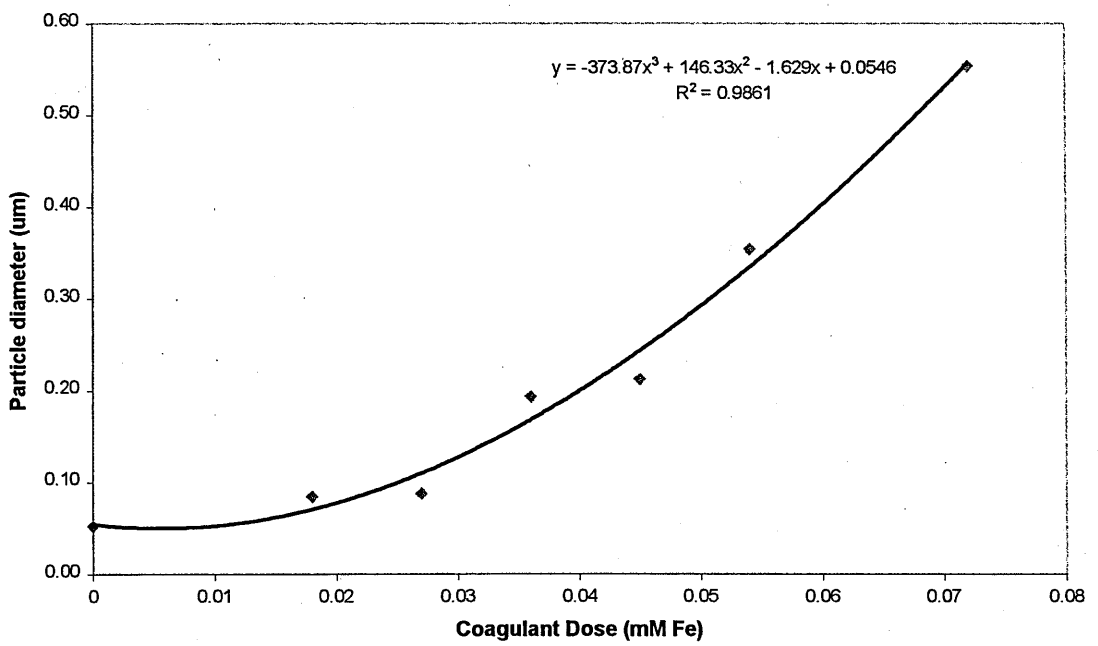

Figure 4.13 Particle diameter for the cake formed between operational cycles, as calculated from *dp/dt* and the Carmen-Kozeny equation

A series of data from filtering poly-aluminium chloride coagulated suspensions through a 47mm 0.2μm Nucleopore filter at different pH values has been presented in the literature by Weisner *et al*, 1989. The system used by the workers was substantially different from the pilot plant used in this study (Table 4.1), both in scale and in configuration: the authors used a single pass system with no backwash or flocculation, which operated at a constant pressure of 1 bar. Most importantly, the flocculation period was 30 minutes – well in excess of any reaction time that could be considered realistic for this application. The data presented by the authors (Figure 4.14), indicate the effects of pH on the filtrate volume transient. This data can be used to plot *(A/V)t* against *(V/A)* (Figure 4.15) to yield $\hat{R}_c$, the specific cake resistance, in

the slope (Figure 4.16). It follows that the mean particle size can once again be estimated from the Carmen-Kozeny equation (Figure 4.17).

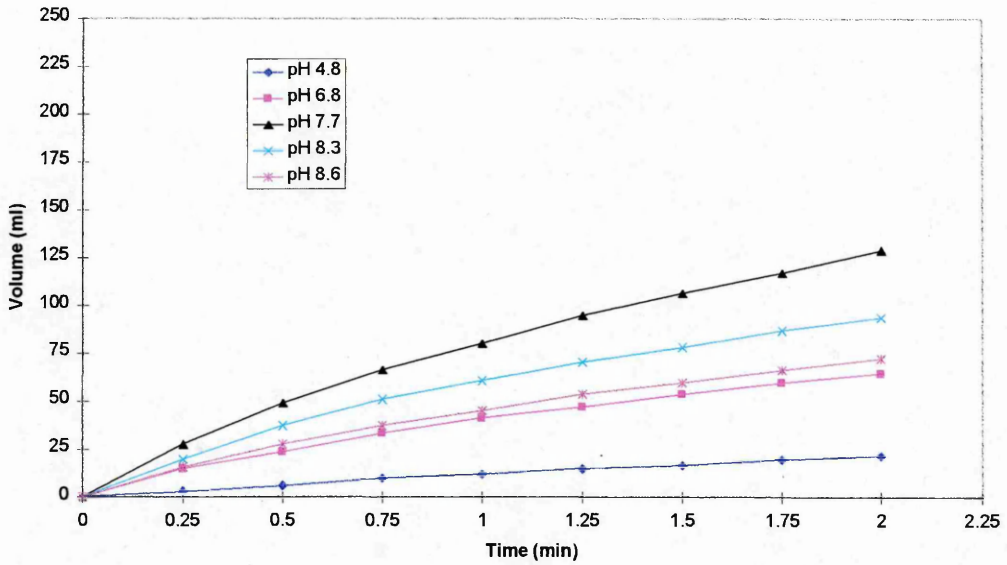

Figure 4.14 Comparison of cumulative filtrate volumes produced over time for suspensions produced at different pH values

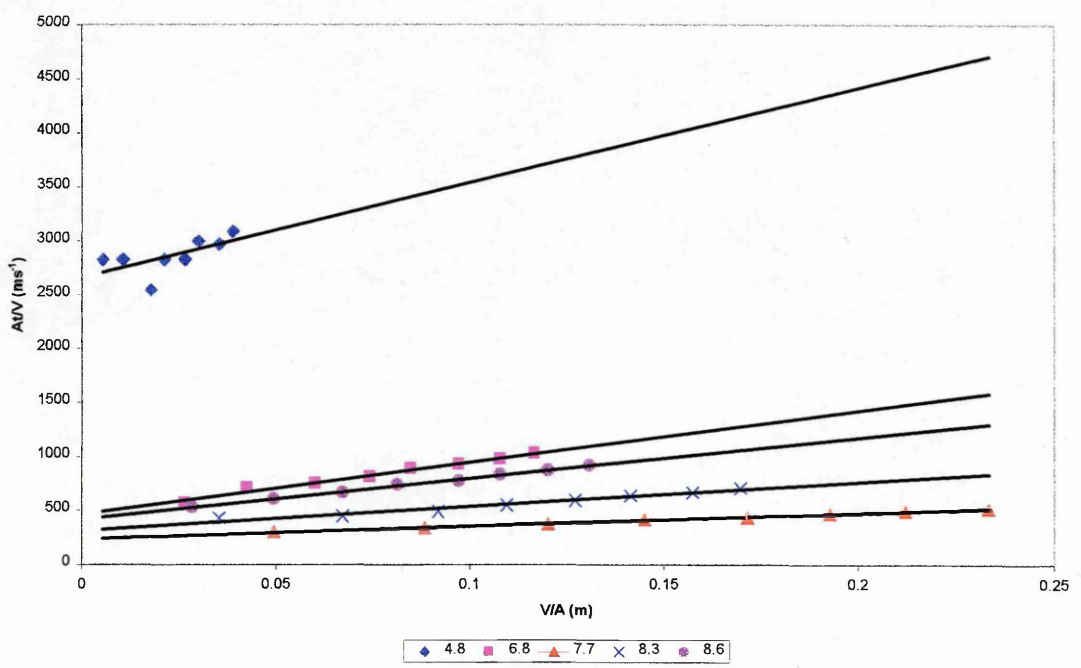

Figure 4.15 *(A/V)t* versus *(V/A)* at different pH values (Weisner *et al*, 1989)

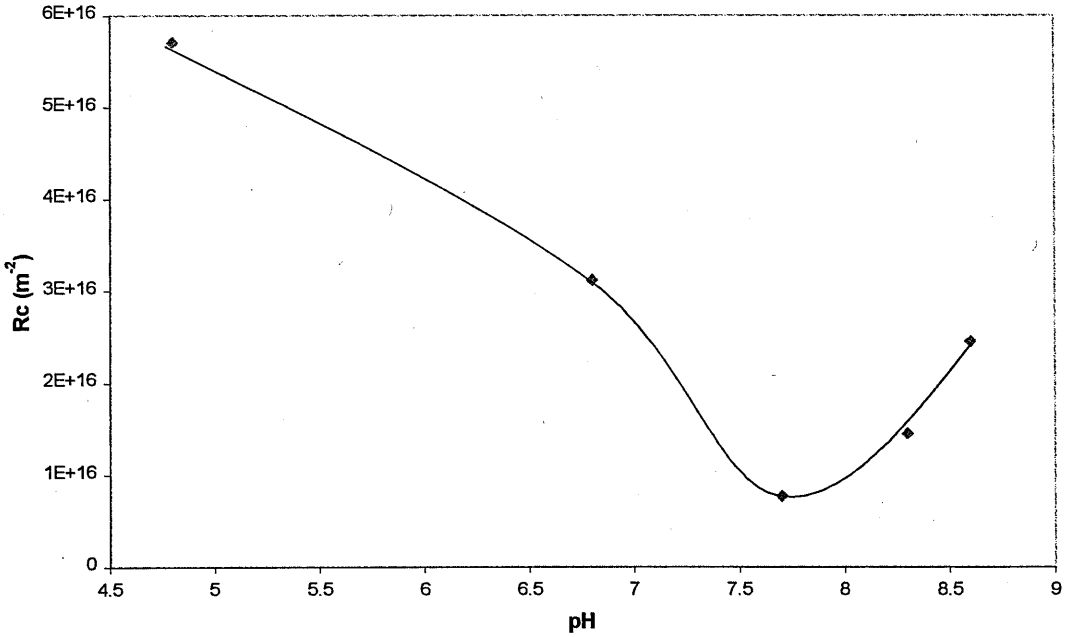

Figure 4.16 $\hat{R}_c$ at different pH values (Weisner *et al*, 1989)

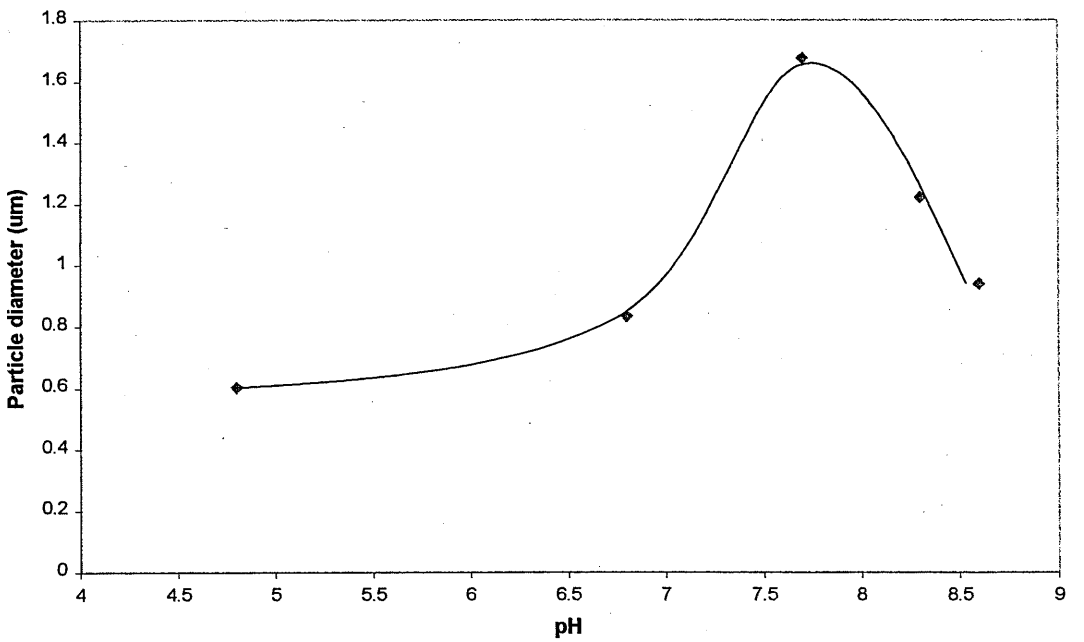

Figure 4.17 Particle size calculated from the Carman-Kozeny equation (Weisner *et al*, 1989).

Weisner *et al* (1989) estimated the size of particles using membranes of various sizes and monitoring pressure build-up, humic acid concentration and laser light scattering measurements of the filtrate. Between pH values 4.8 to 6.0 the measured particle diameter was approximately 0.3μm compared with 0.6μm predicted by the Carman-Kozeny equation (Figure 4.17). At pH 7.7 the measured particle diameter was approximately 1.0μm compared to 1.6μm predicted by the Carman-Kozeny equation (Figure 4.17). In this case the Carman-Kozeny appears to predict the mean particle size with reasonable accuracy. The agreement may be due the fact that the workers were able to directly measure the size of sub-micron particles, which was not possible in the current study.

4.4.1 A comparison of the $\hat{R}_c$ values from Weisner's data and from the current study.

Table 4.1. System variables for two MF systems

System Variable	Hillis	Weisner (1989)
Membrane	Hollow-fibre	Flat sheet
Membrane material	Polysulphone	Polycarbonate
Operational Mode	Constant flow	Constant Pressure
Source	Upland Reservoir	Water analogue
TOC, mg/l	3	10 (Humic acid)
TSS, mg/l	1.5	0
Flux, ms^{-1}	3.06×10^{-5}	1.38×10^{-6} to 1.38×10^{-5}
Specific flux, ms^{-1}/Pa	$4.2 - 10.2 \times 10^{-10}$	$1.38 - 13.8 \times 10^{-11}$
Operating Pressure	30,000 to 70,000 Pa	100,000 Pa
Pore size, μm	0.2	0.2
Membrane Supplier	USF	Nucleopore
Coagulant Concentration	0 to 0.072mM	0.25mM
Coagulant	Fe	Al
Flocculation time, s	20	1800
pH	5.5	4.8 to 6.8

Significant differences exist between the system used in the current study and that of Weisner *et al* (Table 4.1). Despite this the values calculated for $\hat{R}_c$, as shown in Figures 4.12 and 4.16, are of almost the same order of magnitude, 10^{16}-10^{18} m^{-2} for

the constant flux system compared to 10^{15} - 10^{16} m^{-2} for the constant pressure system. Under optimum conditions the minimum cake resistance values measured were 5.9 $x10^{16}$ for the constant flux system compared with 2.37 $x10^{15}$ for the constant pressure system, i.e. just over one order of magnitude difference. These differences may be due to naturally occurring particulate material present in the constant flow system increasing the cake resistance or contributing to pore blockage. The constant pressure system used particle free water, and the cake will have consisted mainly of precipitated aluminium hydroxide since the conditions of coagulation employed were mainly in the sweep coagulation region (Amirtharajah and Mills, 1982). Moreover, the study employed much higher concentrations of coagulant than those used in the current study.

Dosing with coagulant in the current study yielded a 53 fold decrease in $\hat{R}_c$ when the ferric dose was increased from 0.018mM to 0.072mM, compared to a 7 fold decrease when the pH was changed from 4.8 to 7.7 in the Weisner *et al* work (Figures 4.12 and 4.16). There is thus more to be gained from optimising the coagulant dose than from optimising the pH.

The specific resistance values presented in Figure 4.12 for the constant flux system show that the specific resistance of the cake formed during the operational cycle (the transient cake, ($\hat{R}_c$), is about an order of magnitude higher than that for the residual cake ($\hat{R}_c'$), but follows the same trend with coagulant dose. This indicates that the backwash cycle removes more cake or foulant material as the coagulant dose increases, or else that the residual fouling material remaining after a backwash cycle has a lower resistance to filtration.

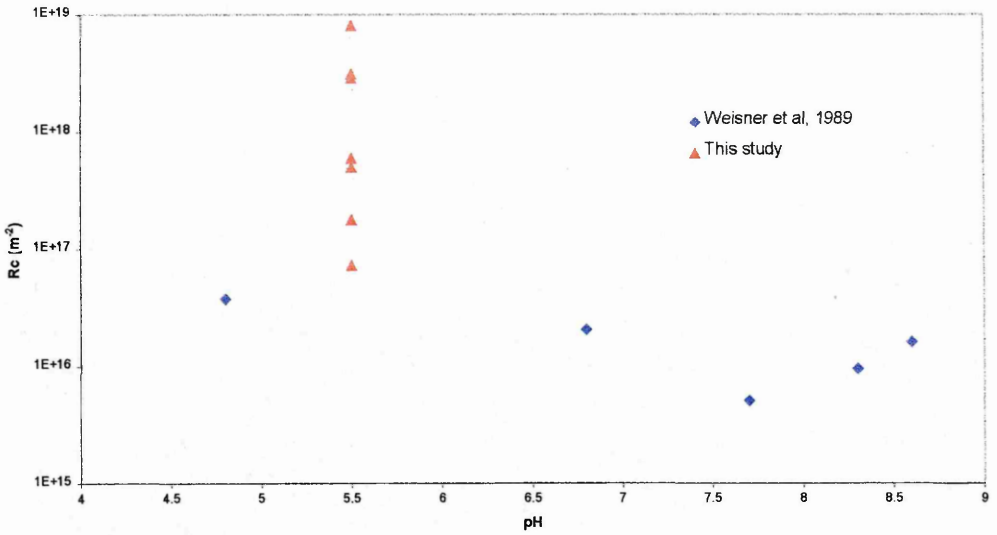

Figure 4.18 $\hat{R}_c$ at different pH values for constant pressure system and constant flow systems

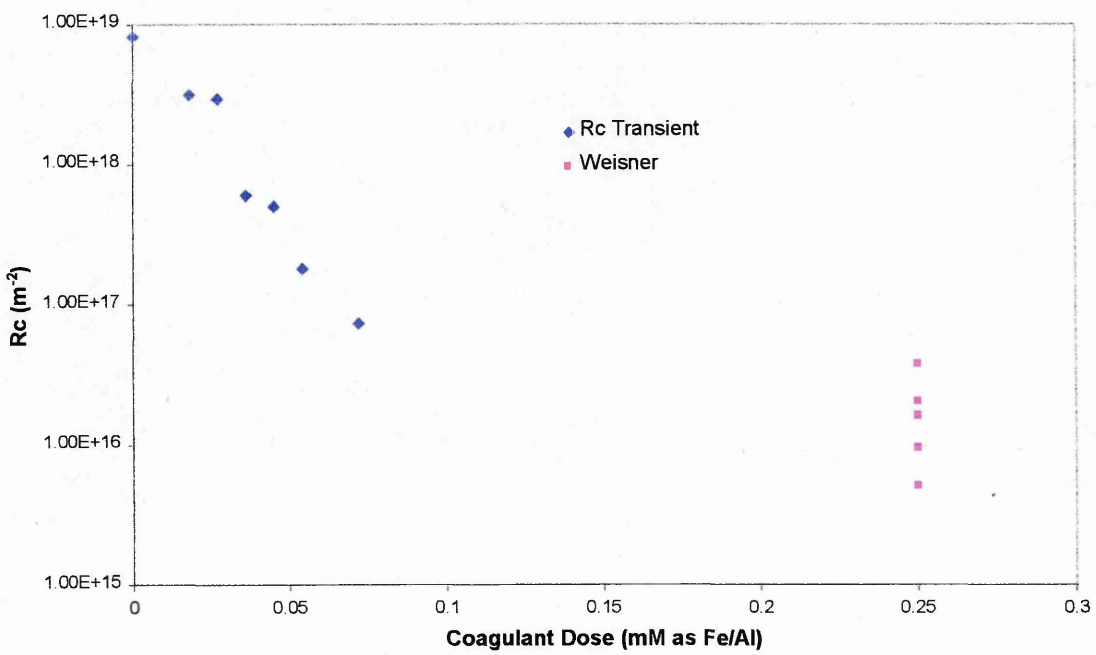

Figure 4.19 $\hat{R}_c$ at different coagulant concentrations for constant flow system and constant pressure systems

Figure 4.18 contains an outlier at pH 4.8, probably in some way associated with a high at a zeta potential (65mV) and the scattered nature of the data in collecting a small volume of filtrate.

Considering the significant differences in the systems employed in this study and that of Weisner *et al*, 1989, i.e. flocculation time, water matrices, coagulant type, membrane configuration and scale the $\hat{R}_c$ values are very similar, especially if the differences in the relative concentrations of coagulant are taken into account. Also, the maximum performance of both systems coincides with the minimum zeta potential. The correlation with Carmen-Kozeny equation differs; this may possibly reflect the limitations of the particle count measurement used in the current study.

5.0 WATER QUALITY

Typical water quality results for raw and permeate water are presented in Table 5.1. The lower concentration of iron in the permeate (20-60μg/l), relative to the raw (50-80μg/l) and coagulated water (up to 4000μg/l), illustrates that the membrane is a robust barrier to the ferric floc. Moreover, the membrane reduced the turbidity to the limit of detection (0.2 NTU) in the permeate from a level of around 1.0NTU, irrespective of the coagulant dose and hence variable particle load in the feed water. The average temperature during the experiments was 5°C.

TOC was also reduced over the coagulant dose range of 0.018 to 0.072mM as Fe. THMFP was reduced, to below 100μg/l, over a coagulant dose range of 0.036 to 0.072mM of Fe. The correlation between ferric dose and percent reduction THMFP is shown in Figure 29. The curve displays a plateau in performance at 0.036mM.

Table 5.1. Water Quality Results for the Microfiltration Pilot Trials, at varying Ferric Doses and a Constant Flocculation Time of 20 Seconds.

Ferric Dose (mM)	Iron (μg/L)		TOC (mg/L)		Turbidity (NTU)		THMFP (μg/l)	
	Raw	Permeate	Raw	Permeate	Raw	Permeate	Raw	Permeate
0	79	40	2.50	2.32	0.9	<0.2	457.8	427.3
0.018	84	68	2.39	1.20	1.6	<0.2	477.2	150.1
0.027	56	37	2.37	1.28	1.3	<0.2	392.9	-
0.036	54	28	2.30	0.76	1.8	<0.2	321.9	82.6
0.045	50	28	2.37	1.37	0.8	<0.2	371.3	63.2
0.054	82	47	2.68	1.23	0.7	<0.2	411.8	97.6
0.072	47	23	2.54	0.65	1.0	<0.2	-	-

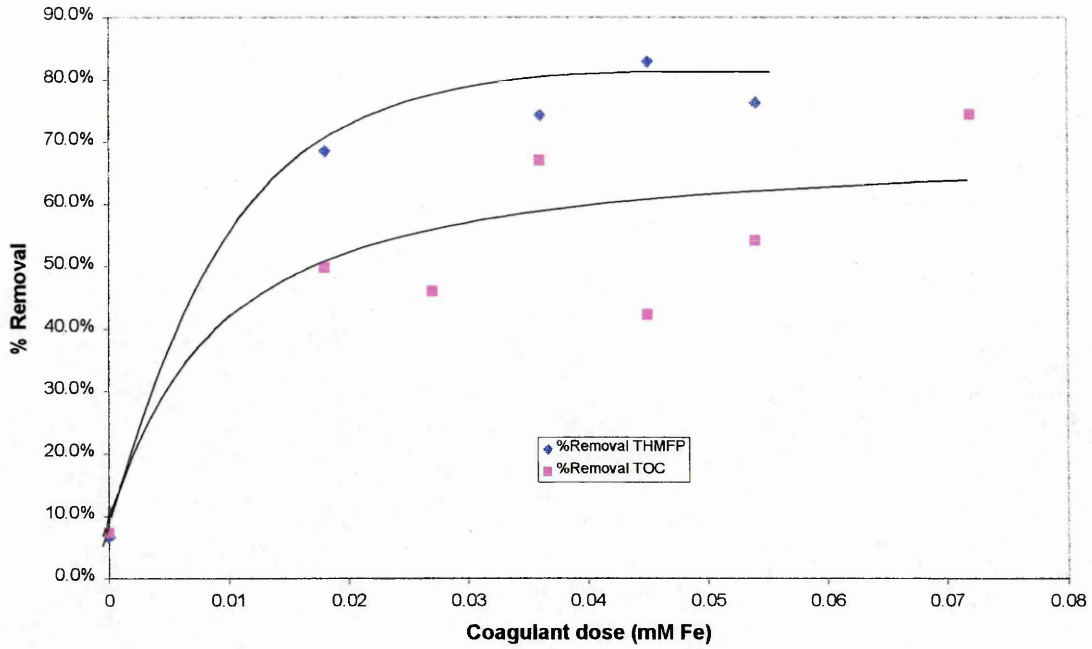

Figure 5.1 %THMFP removal at different coagulant doses (mM of Fe)

THMFP is reduced by approximately 80% at a coagulant concentration of >0.030mM of Fe, this is in agreement with other workers who found that combining coagulation with UF reduces THMFP by 80 to 85% (Clark, 1991). It has been shown that optimised pre-treatment prior to a low-pressure membrane system, such as UF or MF, can be enhanced to remove dissolved organic matter effectively (Laine, 1990).

6.0 CONCLUSIONS

1. A pilot-scale trial of a microfiltration membrane challenged with coagulated raw water has demonstrated trends in cake resistance which have been supported by bench-scale jar tests and zeta potential measurements.

2. Previous work has shown that there to be a substantial effect of pH on permeability of the coagulant filter cake, with reference to alum dosing of humic acid-laden waters under operating conditions of constant pressure. A seven fold decrease in cake resistance from pH 4.8 to 6.8 has been demonstrated (Weisner *et al*, 1989).

3. In the current study the coagulant dose has been shown to substantially alter the nature of the deposit, in that the cake resistance reaches a maximum at a specific low coagulant concentration but decreases substantially at doses above 0.027mM. This trend reflects that higher coagulant doses produce either:

   - a more permeable deposit,
   - a more easily removed deposit, or
   - a combination of the above.

4. The contribution from deposit permeability can be interpreted from the pressure transient over the course of a single cycle. $\hat{R}_c$ was found to decrease by 53 fold from 3.14 x10^{18} to 7.32 x10^{16} m^{-2} when the ferric dose was increased from 0.018mM to 0.072 mM.

5. The resistance of the membrane (R_m) was found to be 7.3 x10^{11}, approximately five orders of magnitude less than the cake formed during an operational cycle under the most favourable coagulation conditions tested.

6. The permeate water quality, in terms of TOC and iron residual, does not change substantially under the range of conditions employed once the optimum coagulant dose (for say, NOM removal) has been reached. This indicates that it is the nature of the deposit that is changed rather than the total quantity of material. Under sub-optimal conditions, there is evident breakthrough of some colloidal/coloured material, indicating a smaller particle size with a correspondingly greater fouling propensity.

7. The rate of particle growth, with respect to the 2-5μm size range (the smallest size fraction determinable), increases linearly with coagulant dose. This supports the view that the optimum dose yields larger particles giving a deposit of greater permeability (given a residence time of 20 seconds).

8. Comparing $dn_{2\text{-}5\mu m}$, the rate of formation of 2 to 5μm particles, with the rate of change of FI with coagulant concentration showed that a threshold value exists, approximately 0.02mM, below which growth of particles is not observed. On the other hand, for FI a near linear response of floc growth, with a positive displacement at zero coagulant dose, probably due to the use of kaolin in the experiments.

9. Zeta potential was found to close to zero for the optimum membrane performance, with respect to residual deposit resistance. This coincides with the maximum rate of particle growth.

10. The combination of coagulation pre-treatment with ferric sulphate and membrane MF has been found to remove about 80% of THMFP. This demonstrates that in terms of water quality objectives the process was found to meet its primary objective.

11. The combination of coagulant pre-treatment and membrane microfiltration offers water quality improvements using low pressure membrane systems that would otherwise require higher pressure systems such as NF.

List of References

Adham, S.S., Jacangelo, J.G., and Laine, J.M., Characteristics and Costs of MF and UF Plants, Journal of the American Water Works Association. May 1996

Anselme, C., Mandra, V., Baudin, I., and Mallevialle, J, Optimum use of Membrane Processes in Drinking Water Treatment, Water Supply, Vol.12, No.1/2, 1994

Badenoch, J., Cryptosporidium in Water Supplies –Report of the Group of Experts, HMSO, London, 1990

Badenoch, J., Cryptosporidium in Water Supplies – Second Report of the Group of Experts, HMSO, London, 1995

Belter, P.A., Cussler, E.L., and Hu, W. -Su, Bioseperations – Downstream Processing for Biotechnology, New York: John Wiley & Sons, 1988

Ben Aim, R., Peuchot, M.M., Vigneswarean, S., Yamaoto and K., Boonthanon, S., A New Process for Water Reuse: In-Line Flocculation-Crossflow Filtration, Proceedings of 2nd IAWPRC Asian Conference on Water Pollution Control, Bangkok, p613-619, 1988

Ben Aim, R., Lui, M.G., and Vigneswaran, S., Recent Developments of Membrane Processes for Water and Wastewater Treatment, Water Science and Technology, Vol.27, No.10, 1993

Boonthanon, S., Prasanthi, H.D., Vigneswaran, S., and Ben Aim, R., Use of a Backflush Technique in Crossflow Microfiltration for Treating Natural Waters and Filter Backwash Wastewater in Water Works, Aqua, Vol.40, No.2, 1991

Bouchier, I., Cryptosporidium in Water Supplies - Third Report of the Group of Experts, HMSO, 1998

Carman, P.C., Fundamental Principles of Industrial Filtration, 1937

Chang, J.S., Tsai, L.J., and Vigneswaran, S., Experimental Investigation of the Effect of Particle Size Distribution of Suspended Particles on Microfiltration, Water Science and Technology, Vol.34, No.9, 1996

Clark, M.M., and Heneghan, K.S., Ultrafiltration of Lake Water for Potable Water Production, Desalination, Vol.80, No.2/3, 1991

Dentel, S.K., Coagulation Control in Water Treatment. Critical Reviews in Environmental Control, Vol. 21 (1), No. 4, 1991

Doshi, M.R., and Trettin, D.R., Ultrafiltration of Colloidal Suspensions and Macromolecular solutions in an Unstirred Batch Cell, Industrial Engineering and Chemical Fundamentals, Vol.20, 1981

Field, R.W., Wu, D., Howell, J.A., and Gupta, B.B., Critical FLUX Concept for Microfiltration Fouling, Journal of Membrane Science 100, 1995

Finch, G.R., Gyurek, L.L., Liyanage, L.R.J., Belosevic, M., Effect of Various Disinfection Methods on the Inactivation of *Cryptosporidium*, American Water Works Association Research Foundation, No. 90734, 1997

Grace, H.P., Resistance and Compressibility of Filter Cakes, Chemical Engineering Programme, Vol.49, 1953

Gregory, J., The Role of Colloid Interactions in Solid-Liquid Separation, Water Science and Technology, Vol. 27, p1-17, 1993

Gregory, J., and Hiller, N., Interpretation of Flocculation Test Data, Proceedings of Filtech Conference, Karlsruhe, Germany, 1995

Haarhof, J. and Cleasby, J.L., Comparing Aluminium and Iron Coagulants for In-Line Filtration of Cold Water, Journal of the American Water Works Association. April 1988

Hahn, T.T., and Stumm, W., Kinetics of Coagulation with Hydrolysed Al(III), Journal of Colloid and Interface Science, 1968

Hall, T, and Hyde, R.A., Water Treatment Processes and Practices, Chapter 33, WRc, 1992

Hillis, P., Colton, J.F., Use of particle monitors to evaluate filter backwash and start-up strategies, Proceedings of Advancing the Science of Water, International Technology Transfer Conference, UKWIR-AWWARF-IWO, Warwick, UK, September 1995.

Holdich, R.G., Constant Pressure Filtration of Clay Effluents Under Non-parabolic Rate Law Conditions, Vol.17, 1996

Hong-Xiao, T. and Stemm, W., The coagulating Behaviours of Fe(III) Polymeric Species – II, Water Research, Vol.21, No.1, 1987

Jacangelo, J.G., DeMarco, J., Owen, D.M., and Randtke, S.J., Selected Processes for Removing NOM: An Overview, Journal of the American Water Works Association, January 1995

Jacangelo, J.G., Laine, J.M., Cummings, E.W., and Adham, S.S., UF with Pre-treatment for Removing DBP Precursors, Journal of the American Water Works Association, May 1995

Jacangelo, J.G., Low Pressure Membrane Filtration for Removal of *Giardia* and Microbial Indicators, Journal of the American Water Works Association, September 1991

Jacangelo, J.G., Patania, N.L., and Laine, J.M., Low Pressure Membrane Filtration for Particle Removal, American Water Works Association Research Foundation, No.89867, 1992

Jacangelo, J.G., The Development of Membrane Technology, Water Supply, Vol.9, No.3/4, 1991

Jacobs, E.P., Botes, J.P., Bradshaw, S.M., and Saayman, H.M., Ultrafiltration in Potable Water Production, Water SA, Vol.23, No.1, 1997

Johnson, P.N. and Amirtharajah, A., Ferric Chloride and Alum as Single and Dual Coagulants, Journal Of The American Water Works Association. Vol.75, No. 3, 1983

Kim, C. -H., Hosoimi, M., Murakami, A., and Okada, M., Characteristics of Fouling Due to Clay-Organic Substances in Potable Water Treatment by Ultrafiltration, Water Science and Technology, Vol.34, No.9, 1996

Kunikane, S., Magara, Y., Itoh, M., Akazawa, H., Nakaoka, C., and Kaburagi, Y., Water Production Performance of thirty-five Different Microfiltartion/Ultrafiltration Systems, Water Supply, Vol.13, Nos.3/4, 1995

Kunikane, S., Magara, Y., Itoh, M., and Tanaka, O., A Comparative Study on the Application of Membrane Technology to Public Water Supply, Journal of Membrane Science 102, 1995

Lahoussine-Turcard, V., Weisner, M.R., Botterro, J.Y., and Mallevialle, J., Coagulation Pre-treatment for Ultrafiltration of a Surface Water, Journal of the American Water Works Association. December 1990

Lahoussine-Turcard, V., Weisner, M.R., Botterro, J.Y., and Mallevialle, J., Coagulation-Flocculation with Aluminium Salts: Influence on the Filtration Efficacy with Microporous Membranes, Water Research, Vol.26, 1992

Lahoussine-Turcaud, V., Jaffres, B., Colombel, P., and Saulnier, A., La Microfiltartion Couplee a la Floculation: Application a la Potabilisation des Eaux Sourterraines en Terrain Karstique, L'Eau, L'Industrie, Les Nuisances, No.146, May 1991

Laine, J.M., Clark, M.M., and Mallevialle, J., Ultrafiltration of Lake Water: Effect of Pre-treatment on the Partitioning of Organics, THMFP and Flux, Journal of the American Water Works Association. December 1990

Letterman, R.D, Quon, J.E., and Gemmell, R.A., Influence of Rapid Mix Parameters on Flocculation, Journal of the American Water Works Association, 1973

Lin, C-F., Huang, Y-J., Hao, O.J., Ultrafiltration processes for removing humic substances: effect of molecular weight fractions and PAC treatment, Water Research, Vol.33, No.5, April 1999.

Magara, Y., Kunikane, S., and Itoh, M., Advanced Membrane Technology for Application to Water Treatment, Water Science and Technology, Vol.37, No.10, 1998

Moulin, C., Bourbigot, M.M., Taz-Pan, A., and Bourdon, F., Design and Performance of Membrane Filtration Installations: Capacity and Product Quality for Drinking Water Applications, Environmental Technology, Vol.12, 1991

Murrer, J., and Holden, P., The use of Ultra Low Pressure Reverse Osmosis Membranes for treating Groundwater, Vol.1, Conference Proceedings of the International Membrane Science and Technology Conference, Sydney, November 1996

Nystrom, M., and Zhu, H., Characterisation of Cleaning Results using Combined Flux and Streaming Potential Methods, Journal of Membrane Science, Vol.131, 1997

Nystrom, M., Determining the Cleaning Efficiency of UF Membranes, Membrane Technology, No.77, 1996

O'Melia, C.R., Review of Coagulation Process, Public Works, Vol.100, Part 5, 1969

Owen, D.M., Amy, G.L., and Chowdury, Z.K., Characterisation of Natural Organic Matter and its Relationship to Treatability, No.89867, AWWA Research Foundation, 1992

Patania, N.L., Jacangelo, J.G., Cummings, L., Wilczak, A., Riley, K., Oppenheimer, J., Optimisation of Filtration for Cyst Removal, American Water Works Association Research Foundation, No.90699, 1995

Pepper, D., Membrane Processes 1966 to 1991, Journal of Chemical Technology and Biotechnology, Vol.55, No.3, 1992

Persson, K.M., and Nilsson, J.L., Fouling Resistance Models in MF and UF, Desalination, Vol.80, No.2/3, 1991

Porter, M.C., What, When and Why of Membranes – MF, UF and RO, What the Filter man Needs to Know About Filtration, AichE Symposium, No.171, 1977

Randtke, S.J., Organic Contaminant Removal by Coagulation and Related Process Combinations, Journal of the American Water Works Association. May 1988

Rebhun, M. and Lurie, M., Control of Organic Matter by Coagulation and Floc Separation, Water Science and Technology, Vol.27, No.11, 1993

Semmens, M.J., and Field, T.K., Coagulation: Experiences in Organics Removal, Journal of the American Water Works Association, August 1980

Shankararaman, C., Jacangelo, J.G., and Bonacquistsi, T.P., Modelling and Experimental Verification of Pilot-Scale Hollow Fibre, Direct Flow Microfiltration with Periodic Backflushing, Environmental Science and Technology, Vol.32, 1998

Sinsaburgh, R.L., Hoehn, R.C., Knock, W.R. and Linkins, A.E., Removal of Dissolved Organic Carbon by Coagulation with Iron Sulphate, Journal of the American Water Works Association. May 1986

Soderbaum, Presentation Speech to Zsigmondy for Nobel Prize in Chemistry, 1925 – http://www.nobel.se/laureates/chemistry-1925-press.html

Solo-Gabriele, H., Neumeister, S., U.S. Outbreaks of cryptosporidiosis, J.A.W.W.A., Vol.88, No.9, September 1996

Taylor, G.S., Hillis, P., and Campbell, A.T., Managing the Risk of Waterborne cryptosporidiosis – Towards Best Practice in the UK, Proceedings of WATERTech Conference, Brisbane, Australia, April 1998

Tambo, N. and Kamei, T., Coagulation and Flocculation on Water Quality Matrix, Water Science and Technology, Vol.37, No.10, 1998

Tarleton, E.S., and Wakeman, R.J., Understanding Flux Decline in Crossflow Microfiltration: Part I – Effects of Particle and Pore Size, Chemical Engineering Research and Design, Vol.71, No.A4, 1993

Taylor, J.S., Membrane Processes for Drinking Water Treatment, Advancing the Science of Water: an International Technology Transfer Conference, UKWIR/AWWARF, Warwick 1995,

Van Houtte, E., Verabauwhede, J., Vanlerberghe, F., de Brujin, F., and Beumer, M., Completing the Water Cycle: Reuse of WWTP Effluent for Drinking Water, Koksijde, Belgium, Proceedings of American Water Works Association and Water Environment Federation Conference - Water Reuse '98, Lake Buena Vista, Florida, February 1998

Vickers, J., Engineering Design Considerations for Microfiltration Systems, Conference Proceedings American Water Works Annual Conference, Vancouver, June 1992

Weisner, M.R., Clark, M.M, and Mallevialle, J., Membrane Filtration of Coagulated Suspensions, Journal of Environmental Engineering, Vol.115, No.1, 1989

Ying, Wei-chi, Duffy and J.J., Tucker, M., Removal of Humic Acid and Toxic Compounds by Iron Precipitation, Environmental Progress, Vol.7, No.4, 1988

Yoo, S., Brown, D.R., Pardini, R.J., and Bentson, G.D., Microfiltration: A Case Study, Journal of the American Water Works Association. March 1995

Yuasa, A., Drinking Water Production by Coagulation-Microfiltartion and Adsorption-Ultrafiltration, Water Science and Technology, Vol.37, No.10, 1998

Bibliography

Ho, W.W., and Sirkar, K.K., Membrane Handbook, Chapman & Hall, New York.

The New Drinking Water Directive, Official Journal of the European Communities, Vol. 41, L330, 98/83/EC, November 1998 (http://europa.eu.int/eur-lex/en/oj/1998/l3019981205en.html)

WHO, Guidelines for Drinking Water Quality, Second Edition, Volume 1, Recommendations, 1993

Water Treatment Membrane Processes, McGraw-Hill, New York

Department of the Environment (DoE), Drinking Water Quality in Public Supplies: An Explanation of the Water Act 1989 and Water Quality Regulations 1989

Everett, D.H., Basic Principles of Colloid Science, Royal Society of Chemistry Paperbacks

APPENDICES

Light obscuration particle counting theory

Light obscuration particle counting has been used for assessing drinking water treatment performance since the early 1980's. The basic working principle of the particle counting sensor is shown below. The sample flows through a sensing zone that is illuminated by a beam of light, usually a laser. When a particle flows through the sensing zone the beam is intersected and some of the light is scattered or adsorbed by the particle resulting in a drop in intensity of the light beam. The change in light intensity is a function of the particle projected area and its refractive index and is measured by the photodetector and this information is processed to produce a particle size (diameter). Light obscuration instruments are capable of measuring particles in the 1 to 500μm size range. The lower limit is determined by the strength of signal that is significantly different to background noise and the upper limit by the size of the sensor region and associated flow appetures through which all particles must pass. The success of the light obscuration particle counter is dependent upon there being only one particle in the light path at any one time. This source of error is minimised by balancing the flow rate through the sensing zone and the diameter of the sensor zone such that only one particle will pass through the zone at any one time.

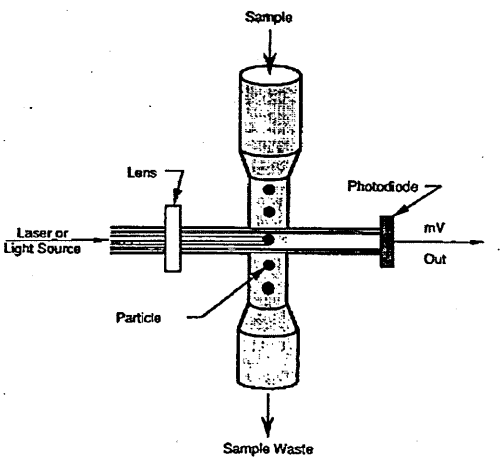

Jar-test, zeta potential and particle count raw data

Jar test results

	Coagulant Dose					
pH	0.036mM	0.045mM	0.054mM	0.036mM	0.045mM	0.054mM
4.12		0.079			0.305	
4.21			0.051			0.311
4.3	0.08			0.31		
4.52		0.022			0.14	
4.75			0.019			0.048
4.92			0.019			0.036
5.05		0.018			0.03	
5.1	0.029			0.025		
5.41		0.023			0.026	
5.55			0.02			0.04
5.68	0.035			0.113		
5.98		0.022			0.028	
6.04			0.025			0.018
6.15	0.039			0.405		
6.38		0.039			0.042	
6.48			0.034			0.026
6.62	0.15			0.95		

Zeta potential data at pH 5.5 for coagulated suspensions, pH 6.7 for raw water.

Coagulant Dose (mM Fe)	pH	Zeta Potential (1)	Zeta Potential (2)	Avg. Zeta Potential
0	6.7	-17.3556	-17.7687	-17.5682
0.036	5.5	-16.2218	-12.1172	-14.1695
0.045	5.5	-9.7005	-8.5508	-9.12565
0.054	5.5	-6.81792	-6.62425	-6.72108
0.072	5.5	-0.1935	-0.2988	-0.24615

Particle count raw data for coagulated suspensions at pH 5.5, – 2 to 5μm particle/ml

Time (S)	0.027mM	0.036mM	0.045mM	0.054mM	0.063mM	0.072mM
2.4	1812	1567	1721	1578	2147	1704
4.8	1779	1576	1577	1716	1962	1818
7.2	1750	1556	1640	1711	1908	1773
9.6	1674	1553	1634	1653	1958	1731
12	1723	1506	1651	1706	2040	1812
14.4	1728	1589	1540	1690	1916	1801
16.8	1693	1557	1614	1604	1869	1814
19.2	1705	1535	1622	1685	1873	1780
21.6	1637	1494	1588	1720	1951	1765
24	1688	1616	1687	1670	1792	1799
26.4	1645	1595	1642	1584	1872	1732
28.8	1755	1524	1644	1631	1816	1742
31.2	1685	1485	1571	1646	1828	1778
33.6	1668	1449	1495	1722	1778	1755
36	1604	1425	1473	1674	1826	1824
38.4	1600	1457	1595	1712	1834	1774
40.8	1606	1413	1566	1650	1811	1793
43.2	1663	1409	1445	1756	1892	1719
45.6	1618	1453	1610	1684	1936	1784
48	1576	1474	1503	1650	1886	1703
50.4	1630	1352	1504	1547	1877	1754
52.8	1697	1500	1546	1678	1871	1764
55.2	1572	1356	1524	1611	1851	1812
57.6	1577	1449	1482	1605	1896	1724
60	1626	1464	1571	1595	1792	1771
62.4	1542	1427	1485	1619	1765	1792
64.8	1602	1523	1562	1538	1775	1814
67.2	1612	1443	1570	1634	1808	1679
69.6	1692	1547	1547	1601	1778	1729
72	1650	1524	1568	1541	1798	1690
74.4	1676	1517	1602	1611	1803	1662
76.8	1683	1526	1658	1667	1809	1714
79.2	1607	1610	1667	1645	1778	1594
81.6	1690	1628	1687	1696	1886	1743
84	1664	1691	1765	1774	1876	1818
86.4	1696	1782	1935	1812	2049	1965
88.8	1778	1922	1992	1913	2171	2227
91.2	1635	2027	2253	2104	2354	2741
93.6	1747	2234	2388	2360	2669	3400
96	1786	2841	2534	2562	3254	4207
98.4	1830	2839	2819	2897	3694	5065
100.8	1912	3153	3140	3342	4346	5796
103.2	2009	3182	3306	3715	4980	6409
105.6	1970	3356	3710	4187	5620	6812
108	1958	3717	3828	4550	5951	7000

110.4	2153	3957	4130	4880	6406	5140
112.8	2255	4226	4400	5159	6293	7364
115.2	2298	4346	4511	5374	6666	6821
117.6	2281	4636	4818	5544	6630	6529
120	2473	4620	5115	5481	6565	6046
122.4	2509	4467	5305	5623	6658	6236
124.8	2805	4931	5418	5802	6163	5749
127.2	2903	5194	5542	5883	4634	5515
129.6	2918	5332	5762	5790	6541	5188
132	3013	5268	5782	5754	6254	4979
134.4	3165	5541	5888	5567	5909	4785
136.8	3231	5583	5653	5668	5729	4679
139.2	3471	5706	6102	5541	5378	4359
141.6	3526	5802	6285	5376	5255	4473
144	3644	5781	5930	5235	4999	4135
146.4	3582	5927	5866	5099	4729	4089
148.8	3683	5938	6274	5120	4711	3895
151.2	3625	5920	6306	5005	2589	3757
153.6	3902	5780	6324	4912	5027	3736
156	3982	5917	6332	4922	4606	3669
158.4	4006	5867	6544	4789	4237	3507
160.8	3936	5757	6572	4767	4172	3438
163.2	4163	5890	6614	4602	3960	3323
165.6	4253	6048	6522	4419	3981	3323
168	4249	5811	6657	4261	3821	3406
170.4	4235	5991	6496	4253	3783	3261
172.8	4195	5955	6413	4268	3646	3295
175.2	4508	5976	6629	4213	3497	3135
177.6	4572	5889	6839	4146	3555	3145
180	4479	5756	6837	4067	3411	3123
182.4	4590	5806	6752	4019	3370	3062
184.8	4428	6009	6888	3926	3214	3019
187.2	4524	6044	6536	3762	3382	2864
189.6	4499	5859	6642	3738	2987	3008
192	4322	5889	6655	3646	3240	2985
194.4	4533	5775	6594	3765	2915	2909
196.8	4605	5826	6677	3708	3046	2948
199.2	4386	5704	6739	3645	3040	2899
201.6	4567	5770	6559	3506	2994	3007
204	4592	5758	6642	3468	2971	2940
206.4	4603	5761	6746	3407	2962	2889
208.8	4520	5718	6461	3313	2824	2982
211.2	4547	5854	6595	3465	2938	2908
213.6	4278	5780	6621	3278	2897	2869
216	4572	5729	6605	3331	2869	2972
218.4	4521	5600	6371	3310	2742	2923
220.8	4360	5625	6692	3198	2966	3056
223.2	4544	5596	6550	2982	3006	2989
225.6	4383	5559	6525	3203	2901	3164
228	4579	5527	6594	3260	2901	2956
230.4	4452	5493	6725	3100	2715	2942

232.8	4438	5639	6508	3088	2715	2994
235.2	4442	5437	6558	3049	2534	2842
237.6	4518	5421	6488	3072	2152	3040
240	4466	5403	6577	3128	3372	2991
242.4	4370	5462	6591	3053	3252	3082
244.8	4401	5468	6732	3093	2953	2946
247.2	4122	5647	6717	2975	3030	2923
249.6	4445	5555	6824	2979	3022	2921
252	4348	5673	6717	3071	3070	3038
254.4	4443	5438	6665	2991	3016	3037
256.8	4240	5327	6515	2864	3004	2915
259.2	4276	5315	6623	3068	2798	3100
261.6	4220	5410	6515	2966	2945	3115
264	4208	5471	6632	2976	2850	3077
266.4	4165	5316	6643	3014	2860	2952
268.8	4204	5449	6786	2953	2861	3036
271.2	4190	5320	6498	2998	2949	3057
273.6	4132	5433	6576	2951	2745	3013
276	4152	5472	6465	2970	2955	3137
278.4	4116	5309	6440	2906	2848	3039
280.8	4116	5437	6456	2932	2747	3029
283.2	4119	5500	6463	2809	2515	3128
285.6	4089	5523	6513	2828	2348	3115
288	4087	5224	6471	2755	2369	3212
290.4	4004	5120	6523	2830	2519	3305
292.8	4003	5234	6300	2850	2428	3164
295.2	3910	5239	6520	2823	2381	3108
297.6	3920	5267	6576	2808	2332	2217
300	4072	5375	6512	2788	2432	3664
302.4	3891	5356	6607	2763	2282	3628
304.8	3942	5387	6475	2819	2414	3351
307.2	3822	5260	6795	2823	2378	3195
309.6	3801	5134	6696	2882	2393	3067
312	3771	5165	6628	2851	2384	3097
314.4	3737	5127	6763	2824	2348	3090
316.8	3824	5137	6638	2805	2369	3054
319.2	3687	5163	6780	2812	2397	3003
321.6	3696	5232	6650	2840	2292	2982
324	3772	5217	6400	2716	2408	2936
326.4	3677	5157	6605	2908	2427	2932
328.8	3610	5247	6559	2828	2460	2975
331.2	3790	5158	6657	2774	2402	3027
333.6	3681	5114	6558	2737	2391	2995
336	3640	5226	6524	2780	2359	2866
338.4	3679	5055	6466	2774	2402	2976
340.8	3669	5121	6630	2767	2485	2954
343.2	3565	5141	6596	2651	2380	3088
345.6	3482	5175	6538	2668	2397	3019
348	3657	5264	6644	2765	2484	3086
350.4	3604	5200	6716	2688	2495	2996
352.8	3609	5121	6925	2822	2407	3121

355.2	3462	5126	6606	2765	2449	3128
357.6	3518	5157	6584	2756	2444	2991
360	3300	5115	6732	2722	2355	3051
362.4	3329	5126	6629	2668	2489	3090
364.8	3856	5174	6707	2748	2417	3063
367.2	3409	5332	6815	2759	2372	3087
369.6	3461	5243	6814	2721	2359	2986
372	3343	5110	6721	2724	2403	3134
374.4	3539	5168	6592	2610	2421	3076
376.8	3326	4966	6782	2665	2451	3136
379.2	3392	4976	6797	2819	2536	3099
381.6	3414	5056	6780	2643	2357	3102
384	3349	5047	6753	2714	2407	2994
386.4	3408	4972	6658	2813	2437	3179
388.8	3306	5026	6697	2717	2395	3188
391.2	3343	4995	6626	2582	2538	3268
393.6	3377	5033	6513	2591	2452	3203
396	3351	5018	6366	2880	2505	3111
398.4	3424	5068	6400	2632	2483	3170
400.8	3334	5019	6652	2822	2619	3166
403.2	3294	4923	6424	2718	2477	3168
405.6	3262	5149	6555	2824	2435	3282
408	3278	5133	6469	2742	2358	3259
410.4	3294	5261	6654	2725	2304	3226
412.8	3126	5204	6475	2544	2432	3328
415.2	3234	5180	6547	2716	2418	3250
417.6	3233	5296	6636	2657	2424	3323
420	3159	5149	6646	2835	2433	3291
422.4	3344	5023	6523	2753	2483	3296
424.8	3243	4839	6588	2619	2408	3255
427.2	3288	5091	6602	2652	2386	3305
429.6	3047	5222	6699	2640	2438	3134
432	3079	5141	6500	2804	2490	3448
434.4	3148	5029	6556	2811	2262	3302
436.8	3135	4834	6539	2952	2396	3326
439.2	3181	5032	6389	2812	2435	3301
441.6	3171	4986	6286	2927	2372	3367
444	3125	5072	6529	2950	2357	3455
446.4	3111	5105	6549	2849	2474	3503

Particle count raw data for filtered de-ionised and raw water- 2 to 5μm particle/ml

	Deionised Water	Raw Water
2.4	170	184
4.8	142	198
7.2	171	189
9.6	147	186
12	142	183
14.4	153	171
16.8	170	189
19.2	162	186
21.6	147	180
24	152	183
26.4	171	161
28.8	150	171
31.2	165	173
33.6	158	186
36	168	181
38.4	170	188
40.8	157	172
43.2	164	197
45.6	174	176
48	169	169
50.4	166	181
52.8	150	162
55.2	164	205
57.6	172	157
60	149	176
62.4	149	169
64.8	166	186
67.2	164	178
69.6	170	208
72	170	157
74.4	142	180
76.8	162	188
79.2	160	209
81.6	158	187
84	174	215
86.4	158	198
88.8	160	187
91.2	167	215
93.6	165	189
96	140	223
98.4	129	203
100.8	162	213
103.2	154	197
105.6	165	199
108	160	218

110.4	163	223
112.8	169	195
115.2	154	215
117.6	126	207
120	190	197
122.4	155	189
124.8	138	203
127.2	160	217
129.6	157	211
132	162	183
134.4	172	185
136.8	166	234
139.2	155	197
141.6	175	213
144	173	223
146.4	167	210
148.8	172	216
151.2	153	202
153.6	164	193
156	160	225
158.4	169	234
160.8	141	216
163.2	178	242
165.6	164	248
168	155	227
170.4	144	223
172.8	145	242
175.2	158	250
177.6	151	265
180	159	245
182.4	168	269
184.8	168	287
187.2	166	276
189.6	168	293
192	167	333
194.4	158	338
196.8	166	347
199.2	152	386
201.6	173	385
204	172	443
206.4	158	511
208.8	160	535
211.2	143	544
213.6	173	652
216	161	672
218.4	168	721
220.8	166	758
223.2	157	812
225.6	135	943
228	179	978
230.4	162	1068

232.8	138	1102
235.2	148	1253
237.6	165	1231
240	147	1332
242.4	162	1491
244.8	174	1568
247.2	137	1683
249.6	164	1638
252	161	1811
254.4	195	1861
256.8	146	1986
259.2	140	2119
261.6	155	2105
264	158	2253
266.4	143	2354
268.8	160	2517
271.2	162	2481
273.6	162	2615
276	162	2798
278.4	149	2769
280.8	169	2875
283.2	148	2987
285.6	163	2997
288	179	3119
290.4	171	3301
292.8	169	3329
295.2	163	3281
297.6	169	3445
300	135	3467
302.4	152	3581
304.8	164	3625
307.2	162	3801
309.6	162	3758
312	158	3743
314.4	152	3995
316.8	165	4059
319.2	174	4136
321.6	149	4102
324	153	4160
326.4	162	4331
328.8	155	4326
331.2	154	4310
333.6	154	4359
336	165	4521
338.4	150	4662
340.8	196	4526
343.2	163	4724
345.6	161	4699
348	157	4746
350.4	151	4771
352.8	172	5009

355.2	160	4819
357.6	144	4965
360	144	4978
362.4	171	5058
364.8	154	4952
367.2	185	4967
369.6	168	5094
372	137	5140
374.4	145	5120
376.8	157	5186
379.2	166	5341
381.6	151	5259
384	175	5343
386.4	174	5379
388.8	153	5274
391.2	161	5439
393.6	188	5441
396	179	5373
398.4	158	5619
400.8	162	5469
403.2	149	5523
405.6	165	5563
408	159	5646
410.4	179	5635
412.8	157	5588
415.2	179	5863
417.6	159	5840
420	168	5735
422.4	173	5778
424.8	145	5708
427.2	163	5766
429.6	144	5798
432	155	5691
434.4	143	5846
436.8	176	5984
439.2	138	6094
441.6	151	6007
444	164	5956
446.4	149	5954
448.8	154	5874
451.2	169	6071
453.6	168	6021
456	160	6121
458.4	151	6206
460.8	118	6008
463.2	181	6135
465.6	151	6123
468	157	6177
470.4	138	6209
472.8	160	6125
475.2	139	6283

477.6	146	6095
480	164	6138
482.4	154	6191
484.8	150	6304
487.2	168	6299
489.6	151	6224
492	154	6263
494.4	193	6311
496.8	153	6310
499.2	180	6269
501.6	173	6364
504	180	6335
506.4	168	6383
508.8	171	6379
511.2	148	6572
513.6	174	6398
516	153	6293
518.4	166	6426
520.8	148	6408
523.2	149	6414
525.6	159	6412
528	176	6514
530.4	159	6403
532.8	150	6419
535.2	155	6416
537.6	180	6490
540	156	6522
542.4	171	6613
544.8	157	6376
547.2	185	6562
549.6	163	6527
552	178	6483
554.4	152	6667
556.8	148	6479
559.2	170	6477
561.6	174	6430
564	170	6518
566.4	172	6481
568.8	144	6526
571.2	144	6703
573.6	151	6597
576	186	6596
578.4	172	6534
580.8	161	6682
583.2	160	6678
585.6	160	6641
588	182	6646
590.4	165	6744
592.8	182	6655
595.2	158	6696
597.6	160	6629

600	190	6720
602.4	138	6733
604.8	154	6654
607.2	152	6837
609.6	178	6752
612	161	6734
614.4	167	6782

Pilot Plant Raw Data

Microfiltration Raw data

Membrane trial, 0.072mM as Fe, pH 5.5, constant flow (110lmh)

	Run1	Run 2
Time (s)	Inlet P (Pa)	Inlet P (Pa)
0	33000	35000
120		35000
180	33000	
240	33000	
360	33000	
420		35000
720	33000	
780	33000	
900		35000
1080	33000	
1320		35000
1920	34000	
2040		35000
2100		35000
2520	34000	
3120		35000
3720	34000	
4620		35000
5100	34000	
5280		35000
5460		36000
5580		36000
6600		36000
6900		36000
7500	34000	
7860	34000	
8220		36000
9720		36000
9780		36000
10680	34000	
10740	35000	
11520	35000	
11520		36000
11760	35000	
12000		36000
13200		36000
15360		36000
15600		36000
18660	35000	
18720	35000	
21060	35000	

21120	35000	
22020	35000	
77040		38000
77100		38000
77820		38000
84720	37000	
85080	37000	
85140	37000	
86400	38000	
86640	38000	
86760	38000	
86820	38000	
88020	39000	
88080	39000	
91500	39000	
95820		39000

Membrane trial, 0.054mM as Fe, pH 5.5, constant flow (110lmh)

	Run1	Run 2	Run 3
Time (s)	Inlet P (Pa)	Inlet P (Pa)	Inlet P (Pa)
0	34000	30000	31000
120	35000		
240	35000	30000	31000
360	35000	30000	31000
480	35000	31000	
480			
540			31000
600		31000	
660	35000		
720		31000	
780	35000		
840		31000	
900	35000		
960		31000	
1020	35000		
1080		31000	
1140	36000		
1200		31000	
1740			31000
1860			31000
2100		31000	
2580	36000		
3300		32000	
3480	36000		
3600			32000
4500		32000	
4560		33000	
5220			33000
5460			32000
5700		33000	32000
6900	37000	33000	32000
7200	37000	33000	32000
8160		34000	33000
14400		37000	35000
16380	40000	37000	36000
69120	58000		
72000	59000	53000	
73800			52000
75600			53000

Membrane trial, 0.0mM as Fe, constant flow (110lmh)

Time (s)	Run1 Inlet P (Pa)	Run 2 Inlet P (Pa)
0	34000	32000
60		32000
120	34000	32000
180	34000	32000
300	34000	32500
540		32500
600		32500
660	34000	
720		33000
780	34500	
1080	34000	
1380		33000
1440		33000
1560	34000	
1620	34500	
1740		33500
1860		33500
2460		34000
3420	35000	
3480	35000	
4680		34500
4740		35500
4920	35000	
4980	36000	
5100		35500
6000	36000	
6720	37000	
7020		36000
7140	37000	
7920	38000	
7980	38500	
8220		37000
8340		38000
8400		38500
8460	39000	
9720	39500	
9960	39500	
10020	40000	
10140		39000
10500		40000
11280	41000	
11820	41000	
12300	41000	
12360	43000	
13380	45000	
13680	45000	
78480		101000
75960	107000	

Membrane trial, 0.018mM as Fe, constant flow (110lmh)

	Run1 Inlet P (Pa)	Run 2 Inlet P (Pa)
Time (s)		
0	35000	30000
120	35000	30000
360	35000	30000
600	36000	31000
660		31000
2460	39000	
2520	40000	34000
2580		34000
2700		36000
3060	40000	
3120	41000	
4680	45000	
4740	45000	
5280		39000
5340		40000
5400		40000
5460	46000	
6780	46000	
6480		41000
6540		42000
6600		44000
8160	48000	
8220	50000	
8640	50000	44000
9000	50000	45000
57600		88000
59400	95000	

Membrane trial, 0.027mM as Fe, constant flow (110lmh)

	Run1 Inlet P (Pa)	Run 2 Inlet P (Pa)
Time (s)		
0	35000	30000
120		30000
180	35000	
600		31000
1020	36000	
1080		31000
1140		32000
1380	36000	
2460	38000	
2400		33000
2520	39000	
4320	41000	36000
5040		36000
5400	42000	
5460	44000	
5700	44000	
5760		38000
5820		38000
75780	102000	
75840	103000	
76080		99000
79740		100000
80580		102000
85740	107000	
92940	109000	

Membrane trial, 0.036mM as Fe, constant flow (110lmh)

	Run1 Inlet P (Pa)	Run 2 Inlet P (Pa)
Time (s)		
0	33000	35000
60		
120		35000
240		
480	33000	
600		
720		35000
1500		
1620	34000	35000
1800		
1860	34000	
1920		
2280	34000	
2760		
2880		38000
3060		
5160	36000	
5400		
5520	36000	
7020		
7080		40000
7200		
7260	38000	
7320		
8700	39000	
82800		
84600		65000
88500		69000

Membrane trial, 0.045mM as Fe, constant flow (110lmh)

	Run1	Run 2	Run 3
Time (s)	Inlet P (Pa)	Inlet P (Pa)	Inlet P (Pa)
0	35000	35000	33000
60	35000	35000	
120			33000
180			33000
240	35000	35000	
300		37000	34000
600	35000		34000
720		38000	
780	35500		
1440	36000	38000	34000
1800		37000	35000
2220	36000		
2580	36000		
2700	37000	38000	36000
3600		39000	36000
4320	38000	39000	
5400		40000	
5700	38000		
6720	39000		
7080			36500
7200	39000		37000
8340	39500	40000	
8400	40000	41000	37500
9000		41000	38000
10140	40000		
10500	40000		
10800		42000	
75420	53000		
75660	54000		
75720			52000
76260			53000
84600		59000	
89040		60000	

Calculation of volume fraction (ϕ_s)

Assume density of solids is 1.5 g/ml

1.5mg/l = 1.5 x10^{-3} g/l

This will have a concentration of 1x10^{-3} ml per 1000ml

Therefore the volume fraction = 1x10^{-6}

Total solids is calculated as follows:

(Coagulant dose mg/l as Fe *2.9) + (mg/l of TOC removed) + (TSS as mg/l in the raw water)

Coagulant Dose		Raw TOC	Permeate TOC	Raw TSS	Permeate TSS	Total Solids	Volume Fraction
mg/l	mM	mg/l	mg/l	mg/l	mg/l	mg/l	
0	0	2.5	2.32	1.4	<1	1.4	9.33333E-07
1	0.018	2.39	1.2	3.2	<1	7.29	2.13333E-06
1.5	0.027	2.37	1.28	2.4	<1	7.84	0.0000016
2	0.036	2.3	0.76	2.2	<1	9.54	1.46667E-06
3	0.045	2.37	1.37	1.8	<1	11.5	0.0000012
3.5	0.054	2.68	1.23	1.2	<1	12.8	0.0000008
4	0.072	2.54	0.65	2.2	<1	15.69	1.46667E-06

Calculation of $\hat{R}_c$,$\hat{R}_c'$ and particle diameter

Temperature of Raw Water =5°C, Viscosity =- 1.519 x10^{-3} kgm^{-1}s^{-1}

Dose (mM)	$\phi_s/(\phi_c - \phi_s)$	dp/dt	$\hat{R}_c$	dp/dt	$\hat{R}_c'$	particle diameter (μm)	particle diameter (μm)
0	1.00E-06	1.67E+01	7.64E+18	0.7143	3.27E+17	0.0541693	0.2616860
0.018	2.27E-06	3.33E+01	6.74E+18	1.7329	3.50E+17	0.0576805	0.2529649
0.027	2.90E-06	3.33E+01	5.27E+18	1.6767	2.65E+17	0.0652383	0.2908658
0.036	3.53E-06	8.33E+00	1.08E+18	0.8209	1.06E+17	0.1440360	0.4588263
0.045	4.17E-06	8.33E+00	9.16E+17	0.5457	6.00E+16	0.1564268	0.6111624
0.054	4.80E-06	3.33E+00	3.18E+17	0.4906	4.68E+16	0.2655342	0.6917973
0.072	6.07E-06	1.67E+00	1.26E+17	0.0963	7.28E+15	0.4215521	1.7554817

Weisner Raw Data

Filtration Experiment Raw Data

TIME	Volume of water filtered (m^3)				
s	pH 4.8	pH 6.8	pH 7.7	pH 8.3	pH 8.6
0	0	0	0	0	0
15	0.00000293	0.00001465	0.00002734	0.00001953	0.00001563
30	0.00000586	0.00002344	0.00004883	0.00003711	0.00002734
45	0.00000977	0.0000332	0.00006641	0.00005078	0.00003711
60	0.00001172	0.00004101	0.00008008	0.00006055	0.00004492
75	0.00001465	0.00004688	0.00009472	0.00007031	0.00005371
90	0.0000166	0.00005371	0.00010645	0.00007813	0.00005957
105	0.00001953	0.00005957	0.00011719	0.00008691	0.00006641
120	0.00002148	0.00006445	0.00012891	0.00009375	0.00007227

	PH 4.8	PH 6.8	PH 7.7	PH 8.3	PH 8.6
(V/A)	(a/v)t	(a/v)t	(a/v)t	(a/v)t	(a/v)t
0.005306	0.785338453				
0.010611	0.785338453				
0.017691	0.70656346				
0.021222	0.785338453				
0.026528	0.785338453				
0.026528		0.15706769			
0.028302					0.14721956
0.030059	0.831701807				
0.035364	0.824746117				
0.035364				0.11782087	
0.038895	0.856998759				
0.042445		0.19633461			
0.049507			0.08416392		
0.049507					0.16832785
0.060118		0.20792545			
0.067198				0.12401195	
0.067198					0.18601792
0.07426		0.22443713			
0.08134					0.20490131
0.084889		0.24541827			
0.08842			0.09424705		
0.091951				0.13594181	
0.097257		0.25705176			
0.097257					0.2142098
0.107868		0.27039268			
0.107868					0.23176515
0.109642				0.15200936	

0.116704		0.28562193			
0.120254			0.10394707		
0.120254					0.24254317
0.127316				0.16363545	
0.130865					0.25471611
0.141476				0.17670869	
0.145007			0.11493715		
0.157374				0.18533301	
0.16976				0.19635556	
0.171517			0.12146546		
0.192757			0.12969704		
0.212205			0.13744596		
0.233427			0.14279989		

Calculation of $\hat{R}_c$ and particle diameter

Slope	$\hat{R}_c$	particle diameter (μm)	particle diameter (μm)
8783.1	3.75829E+16	7.42792E-07	0.742792
4792.3	2.05062E+16	1.02632E-06	1.026322
1183.8	5.06548E+15	2.06498E-06	2.064984
2230	9.54217E+15	1.50454E-06	1.504539
3770.6	1.61344E+16	1.15705E-06	1.157046